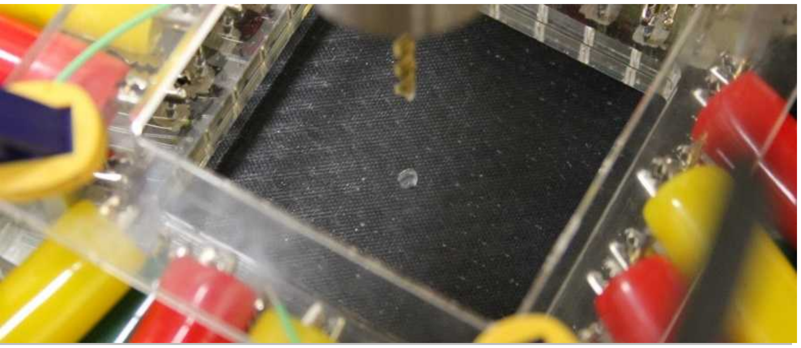

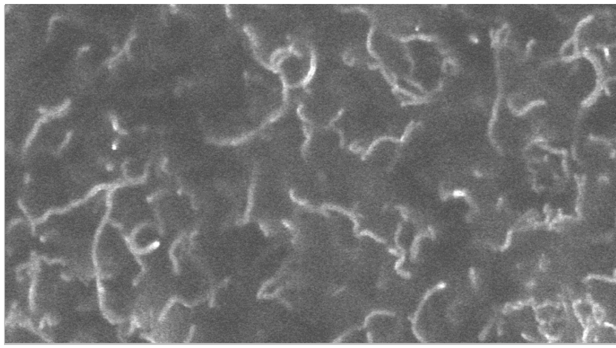

Fiber-Reinforced Polymer Composite Materials: Design, Application, and SHM

Bryan R. Loyola[1]

[1]Sandia National Laboratories, Livermore, CA, USA

U.S. DEPARTMENT OF ENERGY

Sandia National Laboratories is a multi-program laboratory managed and operated by Sandia Corporation, a wholly owned subsidiary of Lockheed Martin Corporation, for the U.S. Department of Energy's National Nuclear Security Administration under contract DE-AC04-94AL85000. SAND NO. 2011-XXXXP

NNSA National Nuclear Security Administration

What Are FRP Composites?

- Composite material: “Composite materials are materials made from two or more constituent materials with significantly different physical or chemical properties, that when combined, produce a material with characteristics different from the individual components.” (Wikipedia)
  - Matrix Material
    - Thermoplastics
    - Epoxies
    - Vinylesters
    - Carbon
    - Metals
    - Concrete
  - Reinforcement Material
    - Carbon
    - Glass
    - Aramids (Kevlar)
    - Polyethylene
    - Cellulose
    - Aluminum
    - Boron
  - Reinforcement Styles
    - Continuous Fiber
    - Woven Fibers
    - Chopped Fibers
    - Particulates

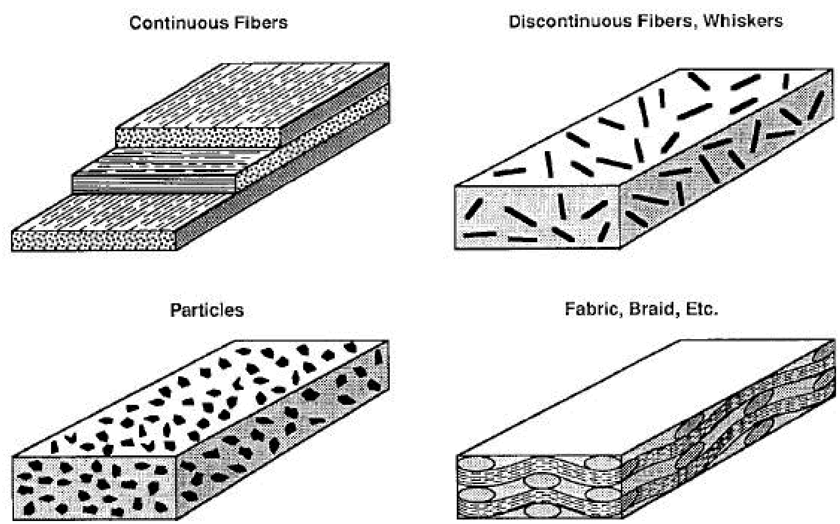

General Composite Properties

- Highly conformable during manufacturing process
- Composite materials do not yield
- Very fatigue resistant
- Age based one humidity conditions
  - Can absorb up to 2 wt% water
- Corrosion resistant, except for carbon and aluminum via galvanic corrosion
- Not sensitive to most standard chemicals
  - Solvents, oils, hydraulic fluids, grease
- Have low to medium impact resistance
- Better fire resistance than light alloys

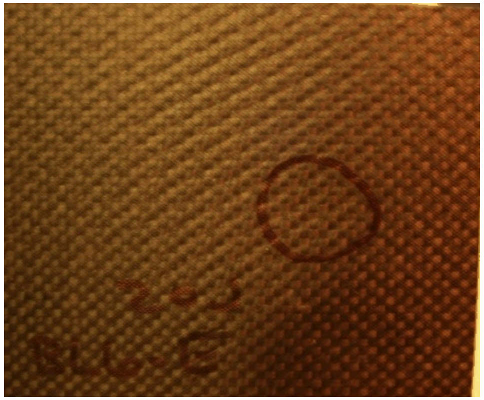

Visual inspection

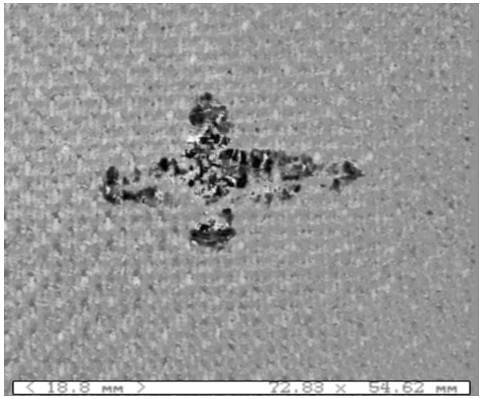

C-SCAN ultrasound image CFRP panel after 20 Joule impact

Material Performance Comparison

Sandia National Laboratories

Material	Steels	Al 2024	Ti 6Al-4V	Carbon/ Epoxy[1]	Glass/ Epoxy[1]	Kevlar/ Epoxy[1]	Boron/ Epoxy[2]
Density [kg/m^3]	7800	2800	4400	1530	2080	1350	1950
Spec. Elastic Modulus [MPa]/ρ	26.3	26.8	23.9	87.6	21.6	63.0	107.7
Poisson Ratio	0.3	0.4	0.3	0.25	0.3	0.34	
Spec. Tensile Strength [kPa] /ρ	205	161	273	830	601	1044	718
Spec. Comp. Strength [kPa] /ρ	397		220	739	289	207	1333
C.T.E. [ppm^{o}C^{-1}]	13	22	8	-1.2	7	-4	5
Temp. Limit [^{o}C]	800	350	700	90	90	90	90

[1]Fiber Volume Fraction = 0.6
[2]Fiber Volume Fraction = 0.5

Carbon Fiber Composite Properties

- Positives
  - High fatigue resistance
  - High heat and electrical conductivity
  - Very high specific elastic modulus
  - High rupture resistance
  - High operating temperatures (limited by epoxy)
- Negatives
  - Delicate fabrication requirements
  - Impact resistance 2-3 times lower than GFRPs
  - Susceptible to lightning strike
- Uses
  - Aircraft main structural support
    - Boeing 787 and Airbus A350 XWB
  - Predominant structural/body material of BMW i3

Boeing 787 Fuselage Nose Section (http://www.nytimes.com)

BMW i3 CFRP Frame (http://www.telegraph.co.uk)

Glass Fiber Composite Properties

- Positives
  - Very good impact resistance
  - Low cost
  - High rupture resistance
  - Very good fatigue resistance
  - Medium maximum operating temperature (846 °C)
    - Limited by resin
- Negatives
  - High elastic elongation
  - Low thermal and electrical conductivity
- Uses
  - Pressure tanks
  - Aircraft wing reinforcement
  - Wind turbine blades

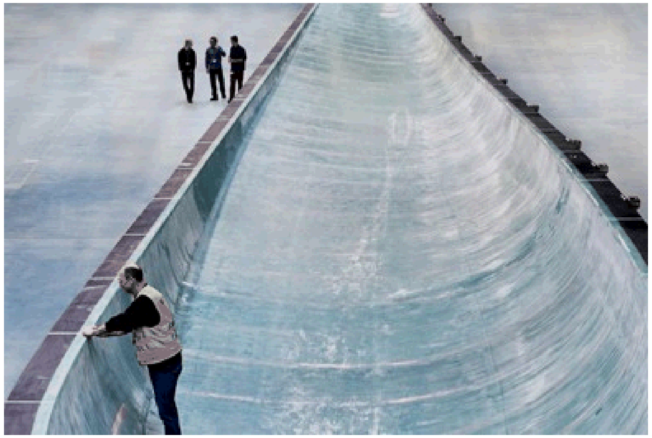

Siemens B75 Glass Fiber Turbine Blade (http://chenected.aiche.org)

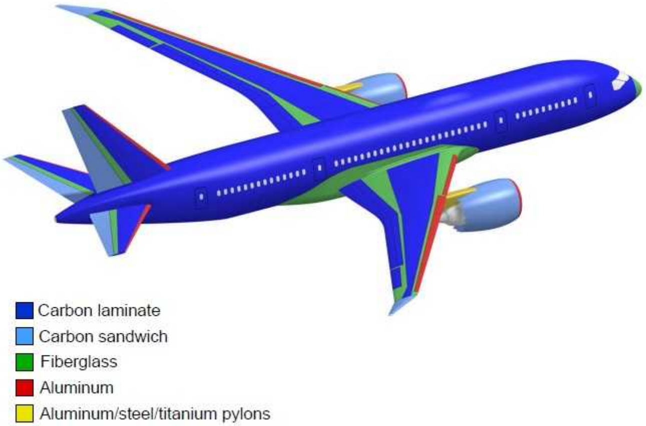

GFRP Usage in Boeing 787 (Green) (Boeing)

CNG Pressure Tank (www.azom.com)

Kevlar/Aramid Fiber Composite Props.

- Positives
  - Very high specific tensile strength
  - Very high impact resistance
  - High rupture resistance
  - Very good fatigue resistance
- Negatives
  - High elastic elongation
    - Need to match appropriately with matrix
  - Low maximum operating temperature
  - Low thermal and electrical conduction
- Uses
  - Pressure tanks (overwrap)
  - Canoes/Kayaks
  - Large yacht, patrol boats, and power boat hulls

Kevlar Constructed Canoe (Wenonah Canoes)

Kevlar Motorcycle helmet

Boron Fiber Composite Properties

- Positives
  - Very high compressive strength
  - Very high tensile stiffness
  - High tensile strength
  - Readily incorporated into metal-matrices (Aluminum)
- Negatives
  - Cost
  - Almost as dense as E-glass
  - Mid-range temperature limit as fiber
  - Higher CTE than carbon
- Uses
  - Ribbed aircraft engine thrust reversers
  - Telescope mirrors
  - Driveshafts for ground transportation

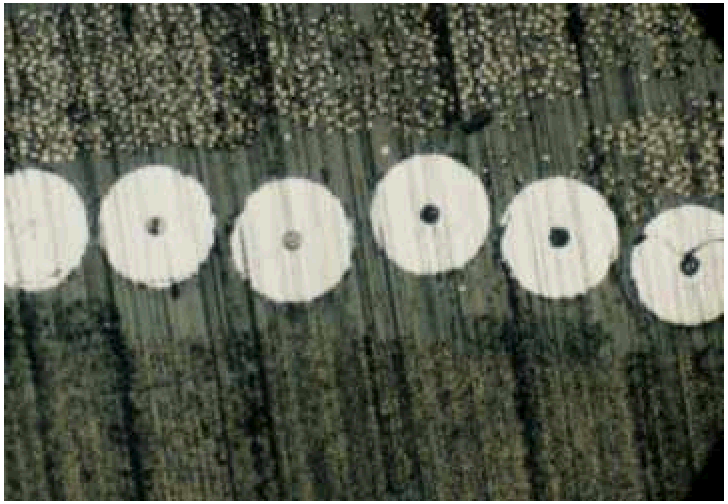

Boron fibers with tungsten cores
www.metallographic.com

Usage of Fiber-Reinforced Composites

Sandia National Laboratories

- Over the past 50 years, increased usage of composite materials

Commercial aircraft systems


Future and legacy spacecraft


Military aircraft

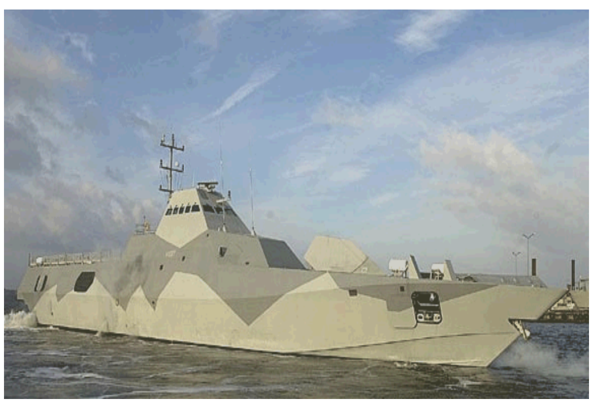
Naval structures


Wind turbine blades


CFRP cable stay bridge

Aircraft Structures

- Benefits
  - Weight-reduction
    - Fuel savings
  - No corrosion
  - Tailorable mechanical properties
    - High hoop strength for fuselage
  - High fatigue resistance
  - Reduce part count
    - Adhesively bonded joints
    - Reduced rivet count
- Typical composite materials
  - Carbon fiber/epoxy
  - Glass fiber/epoxy
  - Boron fiber/epoxy
  - Kevlar fiber/epoxy

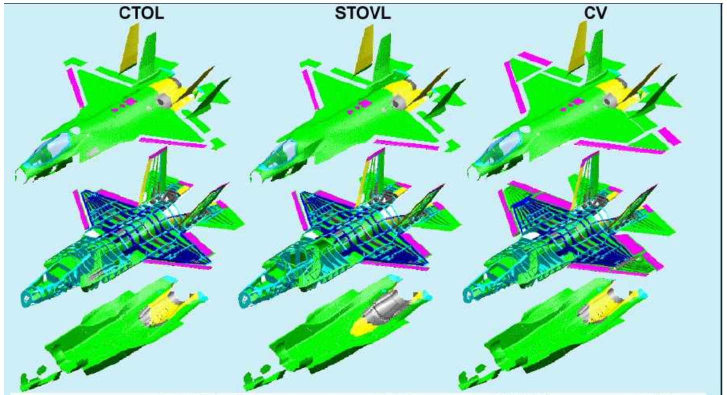

Material	CTOL	STOVL	CV
Aluminum-Lithium	5.2%	4.9%	3.8%
Aluminum	17.9%	16.3%	13.9%
Graphite/Epoxy	32.2%	32.1%	32.8%
Graphite/BMI	2.4%	2.6%	2.4%
Titanium	17.0%	18.7%	17.5%
Steel	11.6%	11.3%	16.9%
Other	13.6%	14.0%	12.7%

Lockheed Martin F-35 JSF material composition (Boeing)

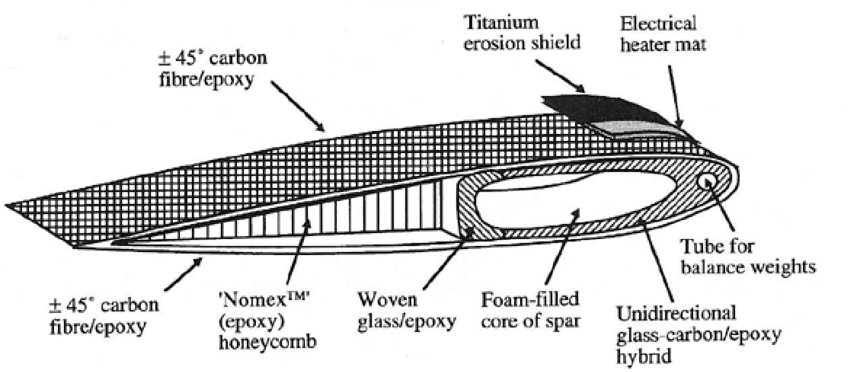

Fig. 12.4 Schematic section through a typical composite construction for a helicopter rotor blade. (Courtesy of Westland Helicopters.)

Boeing 787

- Composites
  - Predominantly CFRP
    - Fuselage
    - Wings
  - GFRP for certain lower-load bearing and impact resistant applications
- Benefits
  - Weight savings
    - Fuel savings
  - Higher fuselage hoop strength
    - Higher cabin pressure in-flight
  - Higher humidity
    - No corrosion, except Al to CFRP
  - Larger windows

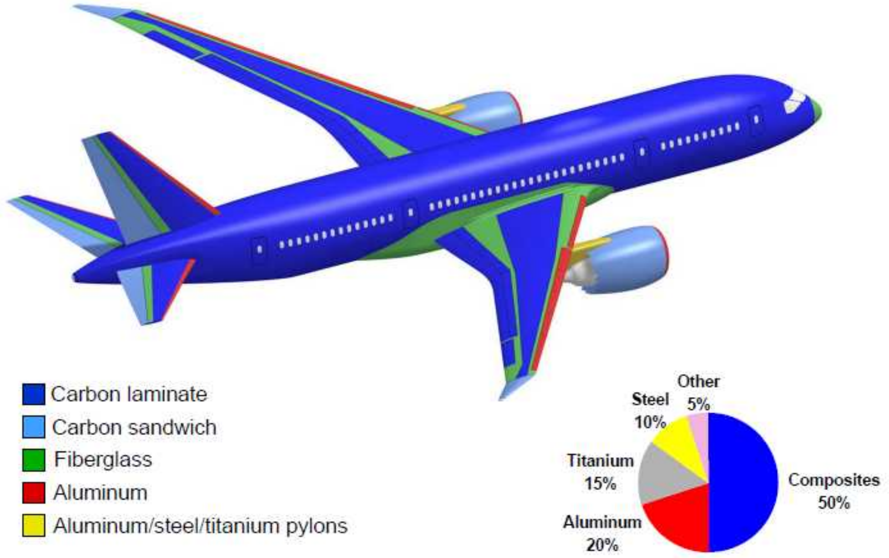

Boeing 787 material composition (Boeing)

Boeing 787 Wing Flex

Smith, 7-April-2011, ESASI-Lisbon | 7

Boeing 787 Wing Flex

Boeing 787 wing on the ground

Boeing 787 wing at cruising altitude (~34,000 ft)

Boeing 737 Wing Flex

Sandia National Laboratories

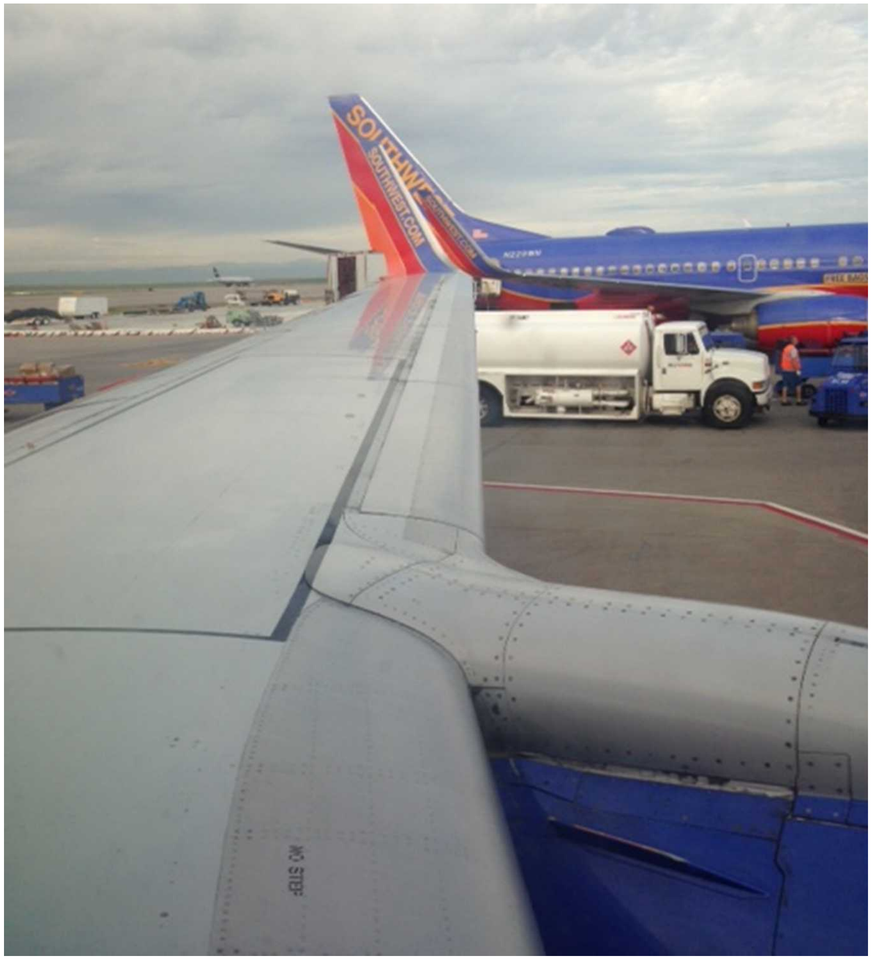

Boeing 737 wing on the ground

Boeing 737 wing on the ground

Space Structures

- Benefits
  - Low CTE
    - High temperature gradients in space
  - Weight reduction
    - Increased cargo capacity
  - Tailorable mechanical properties
  - Tailorable thermal properties
    - Conduct heat from hot to cold side of spacecraft
- Typical composite materials
  - Carbon fiber/epoxy
  - Carbon fiber/phenolic
  - Kevlar fiber/epoxy

Spaceship Two mounted on White Knight Two (Scaled Composites)

James Webb Space Telescope carbon fiber backplane (Hexcel)

Automotive Structures

- Benefits
  - Weight reduction
    - Fuel savings
  - Reduced part count
    - Mostly adhesively bonded joints
  - High fatigue resistance
  - “Cool”-factor
- Typical composite materials
  - Carbon fiber/epoxy
  - Glass fiber/epoxy

Carbon fiber honeycomb on the BWM i3 (Wikipedia)

High-performance car carbon fiber body (Wolf Composites)

Civil Structures

- Benefits
  - Corrosion resistance
  - Fatigue resistance
  - Conformable fabrication
- Typical composite materials
  - Glass fiber/epoxy
  - Carbon fiber/epoxy

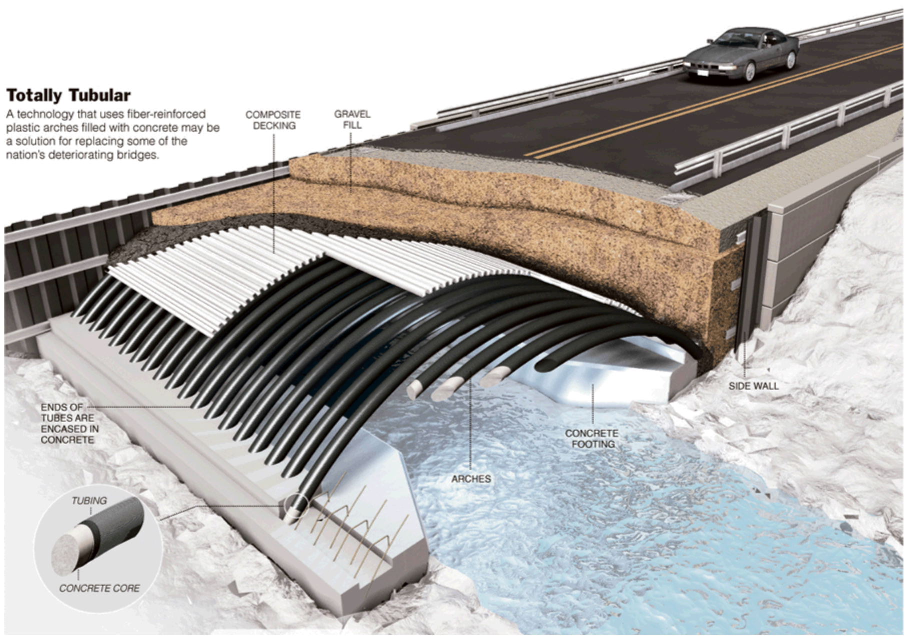

Carbon fiber/glass fiber bridge construction in Pittsfield, Maine (NY Times)

Workers applying GFRP warp to concrete column (Department of Transportation)

Wind Turbines

- Benefits
  - Tailorable laminate properties
  - Cheaper (E-glass)
  - No corrosion
  - Low maintenance

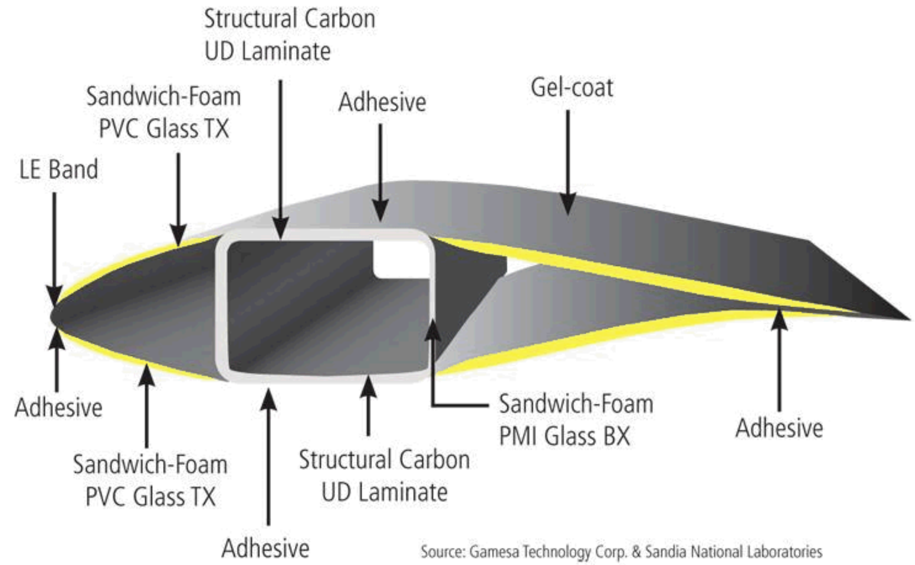

Cross-section of a Gamesa G87/G90 wind turbine blade (Gamesa / Sandia National Laboratories)

Vestas turbine blade mold (MIT Tech Review)

- Typical composite materials
  - Glass fiber/epoxy (current)
  - Carbon fiber/epoxy
    - Reinforcement for GFRP
    - Entire construction

Pressure Vessels

- Benefits
  - High hoop strength
  - Weight savings
- Typical composite materials
  - Glass fiber
  - Kevlar fiber
    - Low-weight/space applications
  - Carbon fiber

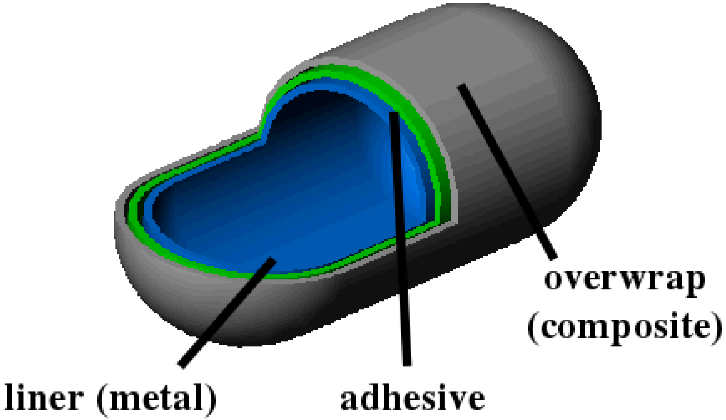

Schematic of a fiber-wound pressure vessel


Kevlar fiber-wound pressure vessel

Composite Manufacturing

- Fabrication
  - Mold-based
  - Fluid diffusion/transfer
  - Mitigation of voids in matrix
- Approaches
  - Autoclave Molding
  - Resin Transfer Molding
  - Vacuum-Assisted Resin Transfer Molding
  - Fiber Winding

Fiber Architectures

- Chopped
  - Loose fibers for toughening polymers
- Tows
  - Bundles of fibers that are continuous
- Tapes
  - Groups of tows configured in tapes for fiber placement
- Mats
  - Typically unidirectional fiber alignment, lacking transverse strength
- Weaves
- 3D Weaves

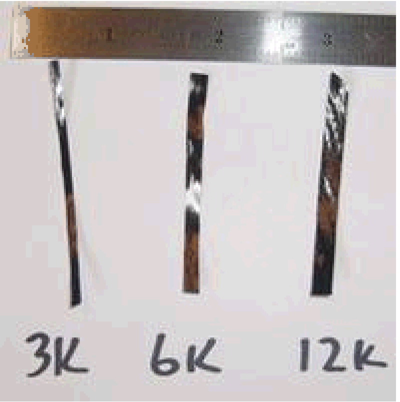

Boeing 787 material composition (Boeing)

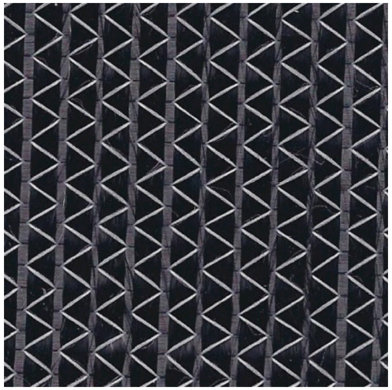

Fiber Weaves

- Plain weave
  - Equal reinforcement
  - High crimp
- Satin weave
  - Much lower crimp
  - Thickness separation of reinforcement
- Twill weave
  - High drape
  - Medium crimp

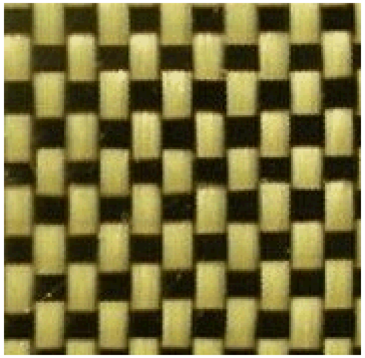

Kevlar/carbon fiber plain weave hybrid

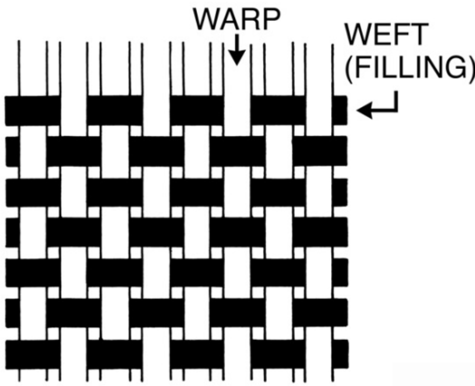

Plain weave (Yates Design)

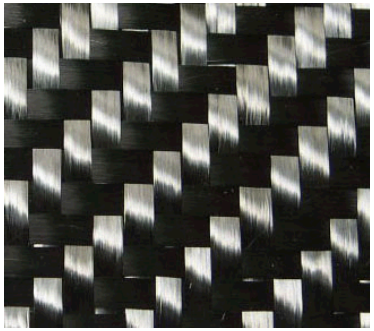

Carbon fiber twill weave

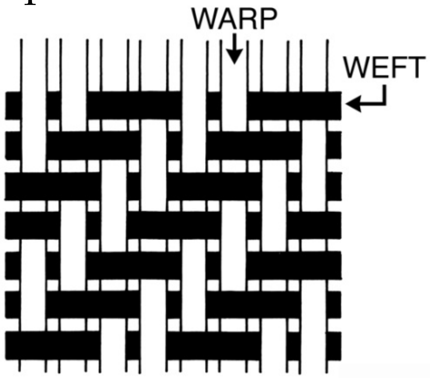

Twill weave (Yates Design)

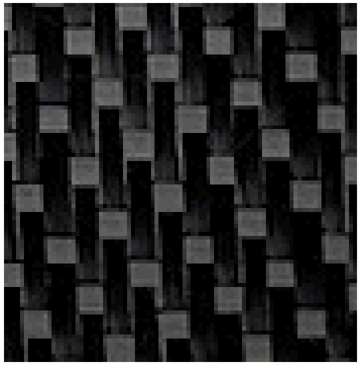

Carbon fiber 5-H satin weave

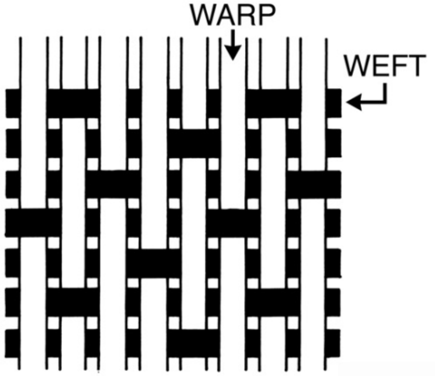

5-harness satin weave (Yates Design)

Autoclave Molding

- Approach
  - Pre-preged materials or hand-wet
  - High temperature
  - Vacuum
    - Remove air from liquid resin
  - Pressure
    - Drive remaining bubbles smaller
- Benefits
  - Low void content
  - Well understood
- Negatives
  - Autoclaves ~100s thousands
  - High pressure hazardous
- Comments
  - Most used approach

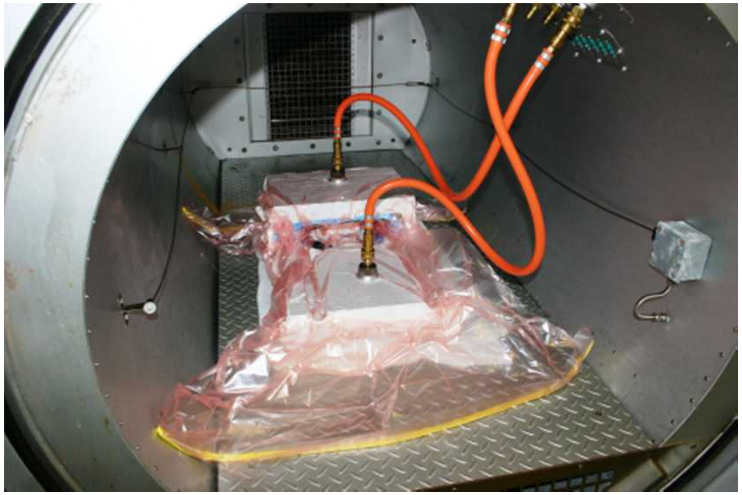

Autoclave with part inside (Wolf Composites)

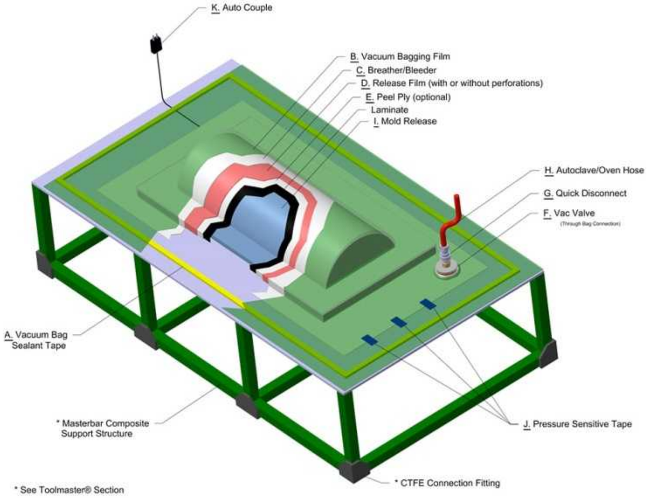

Autoclave molding process (Airtech)

Resin Transfer Molding

- Approach
  - Stack fabric in mold
  - Mix/degas resin
  - Flow resin through fabric
  - Cure under pressure
- Positives
  - Higher toleranced parts
  - Lower void content
- Negatives
  - High mold cost
  - Development time
- Comments
  - Typically used for well dialed in manufacturing

Mold for RTM processing (http://www.keim-fasertechnik.de/)

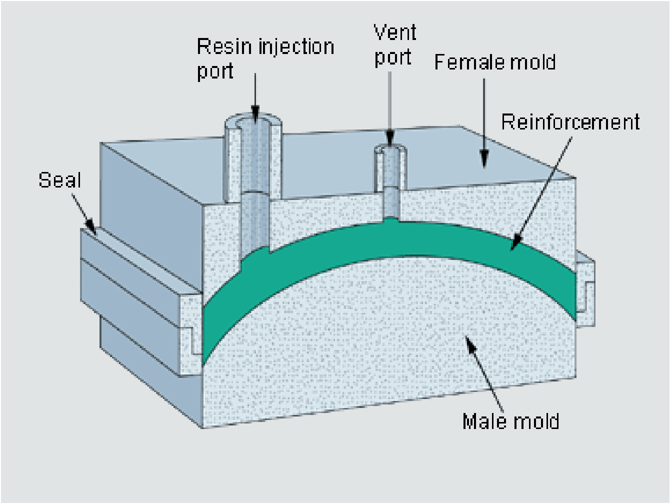

RTM process schematic

Vacuum-Assisted Resin Transfer Molding

- Process
  - Stack fabric
  - Mix/degas resin
- Positives
  - Low cost fabrication
    - Equipment
    - Materials
  - Out-of-autoclave resins

VARTM process to form the hull of a boat

- Negatives
  - Higher void content
  - If vacuum bag fails, whole part wasted
- Comments
  - Great for R&D activities
  - Great for very large parts
    - Wind turbine blades

VARTM part/mold cross-section schematic

Fiber Winding

- Process
  - Fiber tow pulled through resin bath
    - Possibly pre-pregged tape
  - Tow positioned across cylindrical part as mandrel rotated
  - Vacuum-bagged, cured in autoclave or under vacuum
- Positives
  - Rapid manufacturing
  - High hoop strength parts
- Negatives
  - High development time (design)
  - Part cylindrical radius limited (fiber can slip)
- Comments
  - Extensively used for pressure vessels or cylindrical parts

Carbon fiber winding example

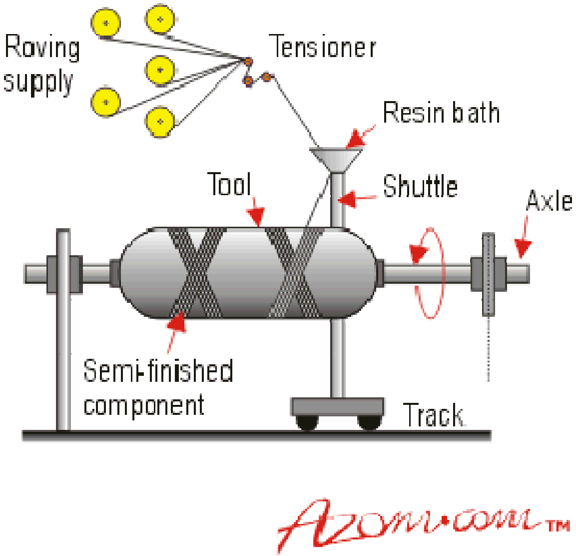

Fiber winding process

Composite Mechanical Performance

- Bottom-up architecture
- Mechanical performance high tailorable
- Factors
  - Material constituent properties
  - Volume fraction of constituents
  - Weave
  - Orientation of fabrics
  - Location of ply orientation in thickness of laminate

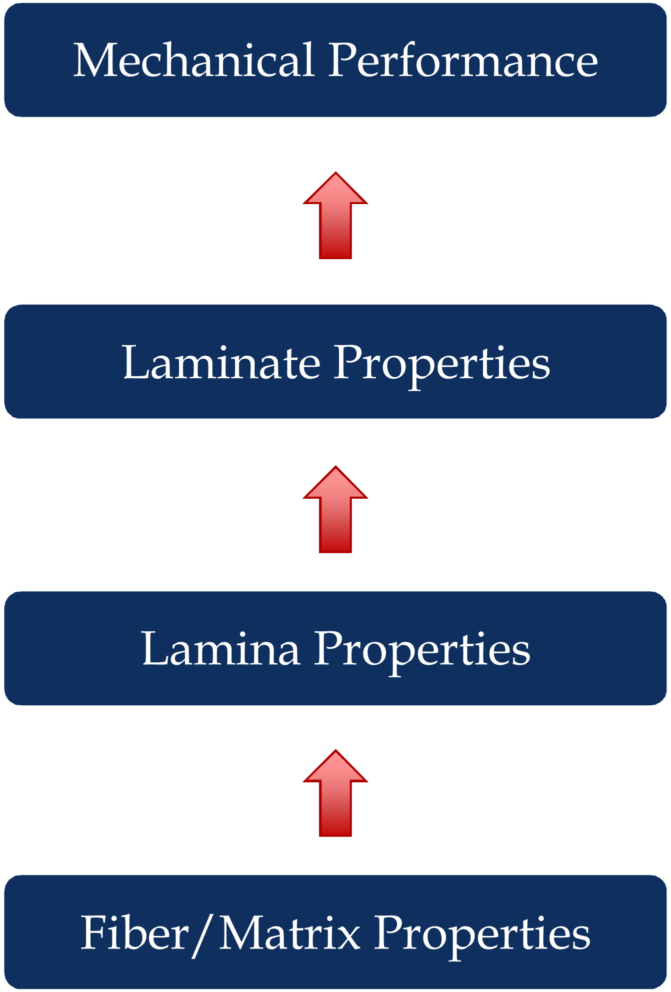

Fiber/Matrix Properties

Material	E-Glass	Carbon	Kevlar 49	Boron	Epoxy	Phenolic	Polyester
Elastic Modulus [GPa]	74.0	230	130	400	4.5	3.0	4
Shear Modulus [GPa]	30.0	50	12	177	1.0	1.1	1.4
Poisson Ratio	0.25	0.3	0.4	0.13	0.4	0.4	0.4
Tensile Strength [MPa]	2500	3200	2900	3400	130	70	80
Ultimate Elongation [%]	3.5	1.3	2.3	0.8	2 @ 100°C	2.5	2.5
C.T.E. [ppm$^{o}C^{-1}$]	5.0	0.2	-2.0	4.0	110	10	80
Temp. Limit [^{o}C]	700	>1500	149	500	90-200	120-200	60-200

Lamina Material Properties

- Need to take constituent properties and make into lamina properties
- Determine properties for longitudinal and transverse directions
  - 1,2,3 notation also used
- Rule of mixture
  - Fiber uniformly distributed
  - Perfect fiber/matrix bonding
  - Matrix is void free
  - Lamina has no residual stress
  - Fiber and matrix are linearly elastic

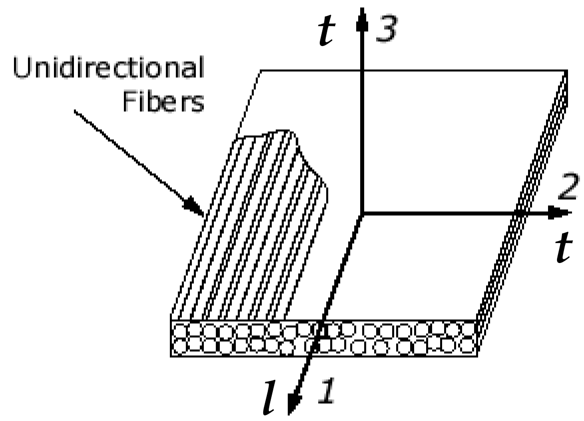

Specific volume representation of a FRP lamina

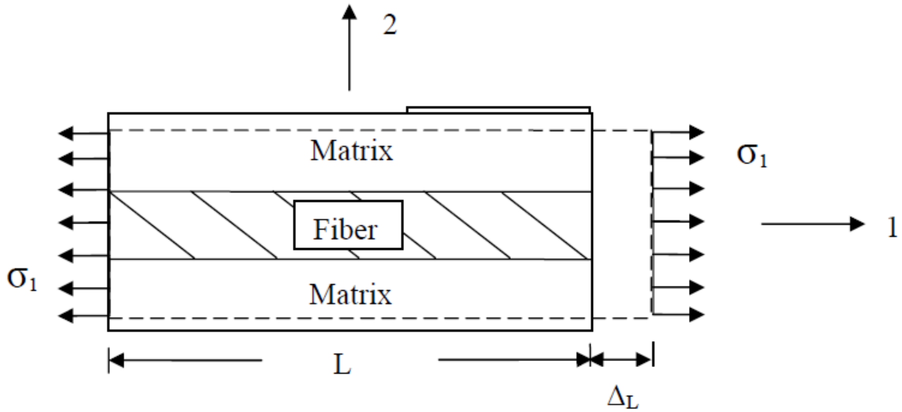

Representative volume of a FRP lamina

Lamina Material Properties

- Longitudinal Tensile Modulus
  - $E_l = V_f E_f + V_m E_m$
- Transverse Tensile Modulus
  - $E_t = E_m \left[\dfrac{1}{(1 - V_f) + \dfrac{E_m}{E_f} V_f} \right]$
- Poisson Ratio
  - $\nu_{lt} = V_f \nu_f + V_m \nu_m$

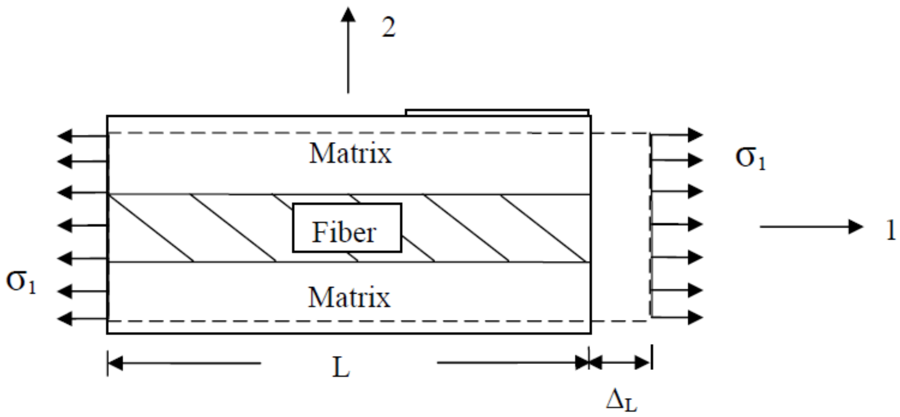

Specific volume representation of a FRP lamina

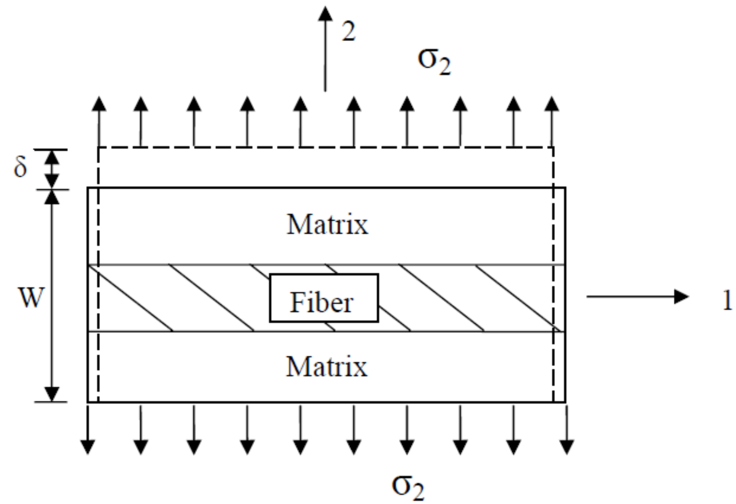

Lamina Material Properties

- Shear Modulus
  - $G_{lt} = G_m \left[\dfrac{1}{(1 - V_f) + \dfrac{G_m}{G_f} V_f} \right]$

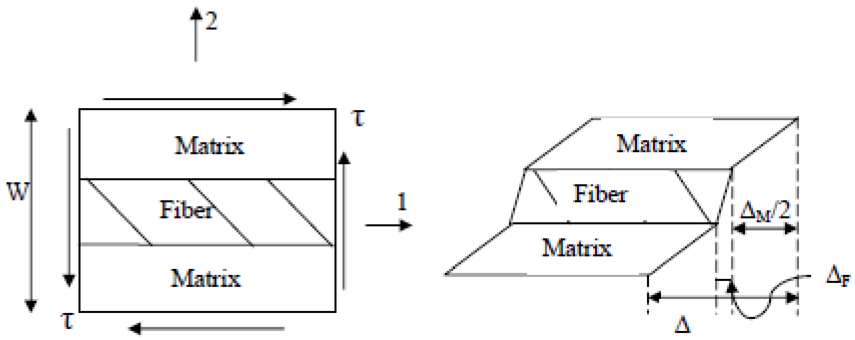

- Longitudinal Coefficient of Thermal Expansion
  - $\alpha_l = \dfrac{\alpha_f E_f V_f + \alpha_m E_m V_m}{E_f V_f + E_m V_m}$
- Transverse Coefficient of Thermal Expansion
  - $\alpha_t = \alpha_m V_m + \alpha_f V_f + \dfrac{\nu_f E_m - \nu_m E_f}{\dfrac{E_m}{\nu_f} + \dfrac{E_f}{\nu_m}} \cdot (\alpha_f - \alpha_m)$

Laminate Stack Sequences

- Nomenclature
  - $[0/+45/90/-45]_{NS}$
  - / - separates each ply
    - Subscript the number of that ply orientation in a row
  - Subscript N indicates how many times this layup sequence is repeated in the stackup
  - S means symmetric about the neutral axis

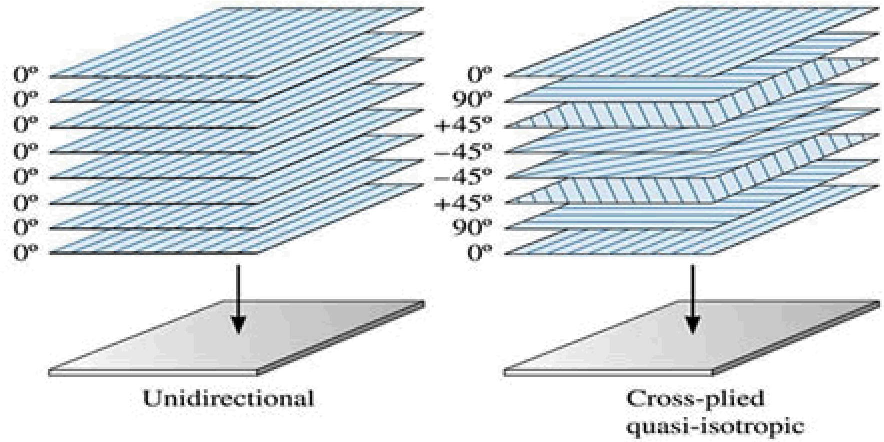

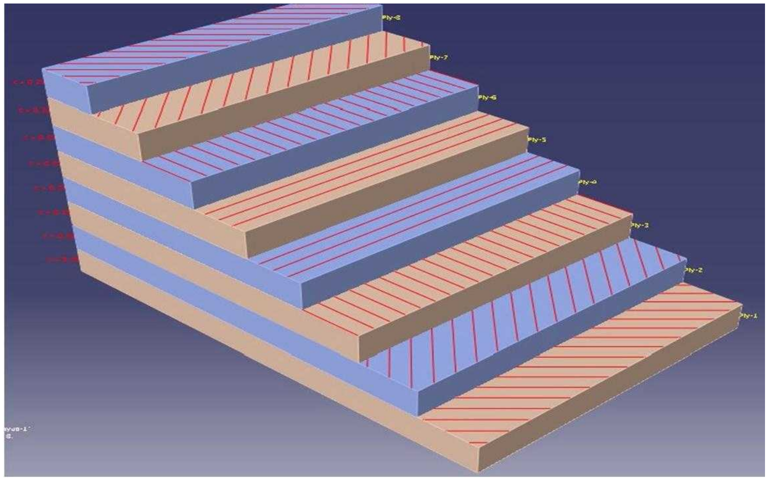

Lamina Mechanical Properties

$$\begin{Bmatrix} \sigma_x \\ \sigma_y \\ \tau_{xy} \end{Bmatrix} = \begin{bmatrix} \overline{E}_{11} & \overline{E}_{12} & \overline{E}_{13} \\ \overline{E}_{21} & \overline{E}_{22} & \overline{E}_{23} \\ \overline{E}_{31} & \overline{E}_{32} & \overline{E}_{33} \end{bmatrix} \begin{Bmatrix} \varepsilon_x \\ \varepsilon_y \\ \gamma_{xy} \end{Bmatrix} - \Delta T \begin{Bmatrix} \overline{\alpha}\overline{E}_1 \\ \overline{\alpha}\overline{E}_2 \\ \overline{\alpha}\overline{E}_3 \end{Bmatrix}$$

$$\overline{E}_{11} = \overline{E}_l \cos^4\theta + \overline{E}_t \sin^4\theta + 2\cos^2\theta \sin^2\theta \left(\nu_{tl}\overline{E}_l + 2G_{lt}\right)$$

$$\overline{E}_{22} = \overline{E}_l \sin^4\theta + \overline{E}_t \cos^4\theta + 2\cos^2\theta \sin^2\theta \left(\nu_{tl}\overline{E}_l + 2G_{lt}\right)$$

$$\overline{E}_{33} = \cos^2\theta \sin^2\theta \left(\overline{E}_l + \overline{E}_t - 2\nu_{tl}E_l\right) + \left(\cos^2\theta - \sin^2\theta\right)G_{lt}$$

$$\overline{E}_{12} = \cos^2\theta \sin^2\theta \left(\overline{E}_l + \overline{E}_t - 4G_{lt}\right) + \left(\cos^2\theta + \sin^2\theta\right)\nu_{tl}\overline{E}_l$$

$$\overline{E}_{13} = -\cos\theta \sin\theta \left[\overline{E}_l \cos^2\theta - \overline{E}_t \sin^2\theta - \left(\cos^2\theta - \sin^2\theta\right)\left(\nu_{tl}\overline{E}_l + 2G_{lt}\right)\right]$$

$$\overline{E}_{23} = -\cos\theta \sin\theta \left[\overline{E}_l \sin^2\theta - \overline{E}_t \cos^2\theta + \left(\cos^2\theta - \sin^2\theta\right)\left(\nu_{tl}\overline{E}_l + 2G_{lt}\right)\right]$$

$$\overline{E}_l = \frac{E_l}{1-\nu_{lt}\nu_{tl}}, \overline{E}_t = \frac{E_t}{1-\nu_{lt}\nu_{tl}}$$

$$\overline{\alpha}\overline{E}_1 = \overline{E}_l \cos^2\theta \left(\alpha_l + \nu_{tl}\alpha_t\right) + \overline{E}_t \sin^2\theta \left(\alpha_t + \nu_{lt}\alpha_l\right)$$

$$\overline{\alpha}\overline{E}_2 = \overline{E}_l \sin^2\theta \left(\alpha_l + \nu_{tl}\alpha_t\right) + \overline{E}_t \cos^2\theta \left(\alpha_t + \nu_{lt}\alpha_l\right)$$

$$\overline{\alpha}\overline{E}_3 = \cos\theta \sin\theta \left[\overline{E}_l\left(\alpha_t + \nu_{lt}\alpha_l\right) + \overline{E}_t\left(\alpha_l + \nu_{tl}\alpha_t\right)\right]$$

Laminate Mechanical Properties

- Symmetric laminates
  - Pure in-plane contributions to in-plane strain

$$\begin{Bmatrix} N_x \\ N_y \\ T_{xy} \end{Bmatrix} = \begin{bmatrix} A_{11} & A_{12} & A_{13} \\ A_{21} & A_{22} & A_{23} \\ A_{31} & A_{32} & A_{33} \end{bmatrix} \begin{Bmatrix} \varepsilon_{0x} \\ \varepsilon_{0y} \\ \gamma_{0xy} \end{Bmatrix} - \Delta T \begin{Bmatrix} \langle \alpha E h \rangle_x \\ \langle \alpha E h \rangle_y \\ \langle \alpha E h \rangle_{xy} \end{Bmatrix}$$

$$A_{ij} = \sum_{k=1^{st}_{ply}}^{N_{plies}} \overline{E}_{ij} t_k = A_{ji}$$

$$\langle \alpha E h \rangle_x = \sum_{k=1^{st}_{ply}}^{N_{plies}} \overline{\alpha} \overline{E}_1^k t_k, \langle \alpha E h \rangle_y = \sum_{k=1^{st}_{ply}}^{N_{plies}} \overline{\alpha} \overline{E}_2^k t_k, \langle \alpha E h \rangle_{xy} = \sum_{k=1^{st}_{ply}}^{N_{plies}} \overline{\alpha} \overline{E}_3^k t_k$$

Laminate Mechanical Properties

- Bending
  - Stiffness comes from outer plies, predominantly
  - Pure bending contributions to flexure

$$\begin{Bmatrix} M_y \\ -M_x \\ -M_{xy} \end{Bmatrix} = \begin{bmatrix} C_{11} & C_{12} & C_{13} \\ C_{21} & C_{22} & C_{23} \\ C_{31} & C_{32} & C_{33} \end{bmatrix} \begin{Bmatrix} \dfrac{\partial^2 w_0}{\partial x^2} \\ -\dfrac{\partial^2 w_0}{\partial y^2} \\ -2\dfrac{\partial^2 w_0}{\partial x \partial y} \end{Bmatrix}$$

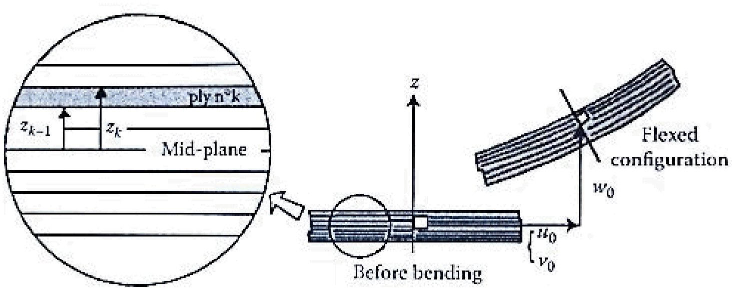

$$C_{ij} = \sum_{k=1^{st}_{ply}}^{N_{plies}} \overline{E}_{k,ij} \frac{\left(z_k^3 - z_{k-1}^3\right)}{3} = C_{ji}$$

Non-Symmetric Laminates

- What happens if the laminate is not symmetric?
  - In-plane/bending coupling is no longer zero
  - Bending CTE is no longer zero

$$B_{ij} = \sum_{k=1^{st}_{ply}}^{N_{plies}} \overline{E}_{ij}^{k} \left(\frac{z_k^2 - z_{k-1}^2}{2} \right)$$

$$\left\langle \alpha E h^2 \right\rangle_x = \sum_{k=1^{st}_{ply}}^{N_{plies}} \overline{\alpha} \overline{E}_1^{k} \left(\frac{z_k^2 - z_{k-1}^2}{2} \right)$$

$$\left\langle \alpha E h^2 \right\rangle_y = \sum_{k=1^{st}_{ply}}^{N_{plies}} \overline{\alpha} \overline{E}_2^{k} \left(\frac{z_k^2 - z_{k-1}^2}{2} \right)$$

$$\left\langle \alpha E h^2 \right\rangle_{xy} = \sum_{k=1^{st}_{ply}}^{N_{plies}} \overline{\alpha} \overline{E}_3^{k} \left(\frac{z_k^2 - z_{k-1}^2}{2} \right)$$

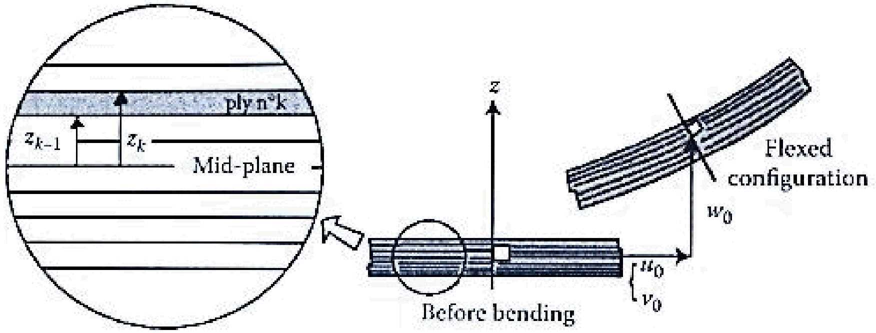

Non-Symmetric Laminates

- In-plane/bending contributions are now non-zero
  - Full matrix would be even larger when taking into account z axis as well
  - Non-symmetric laminates tend to have warpage after cure due to residual stress from epoxy lock-in during current

$$\begin{Bmatrix} N_x \\ N_y \\ T_{xy} \\ M_y \\ -M_x \\ -M_{xy} \end{Bmatrix} = \begin{bmatrix} A_{11} & A_{12} & A_{13} & B_{11} & B_{12} & B_{13} \\ A_{21} & A_{22} & A_{23} & B_{21} & B_{22} & B_{23} \\ A_{31} & A_{32} & A_{33} & B_{31} & B_{32} & B_{33} \\ B_{11} & B_{12} & B_{13} & C_{11} & C_{12} & C_{13} \\ B_{21} & B_{22} & B_{23} & C_{21} & C_{22} & C_{23} \\ B_{31} & B_{32} & B_{33} & C_{31} & C_{32} & C_{33} \end{bmatrix} \begin{Bmatrix} \varepsilon_{0x} \\ \varepsilon_{0y} \\ \gamma_{0xy} \\ \dfrac{\partial^2 w_0}{\partial x^2} \\ -\dfrac{\partial^2 w_0}{\partial y^2} \\ -2\dfrac{\partial^2 w_0}{\partial x \partial y} \end{Bmatrix} - \Delta T \begin{Bmatrix} \langle \alpha E h \rangle_x \\ \langle \alpha E h \rangle_y \\ \langle \alpha E h \rangle_{xy} \\ \langle \alpha E h^2 \rangle_x \\ \langle \alpha E h^2 \rangle_y \\ \langle \alpha E h^2 \rangle_{xy} \end{Bmatrix}$$

Composite Damage Modes

- Susceptible to damage due to:
  - Strain, impact, chemical penetrants, multi-axial fatigue
- Damage modes:
  - Matrix cracking
  - Fiber-breakage
  - Delamination
  - Transverse cracking
  - Fiber-matrix debonding
  - Matrix degradation
  - Blistering
- Difficult to detect
  - Internal to laminate structure
  - Nearly invisible to naked eye
  - Current methods are laborious

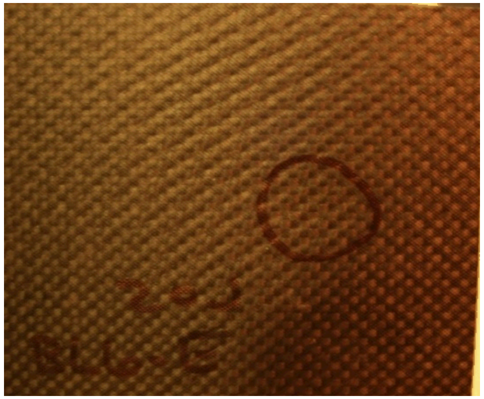

Visual inspection

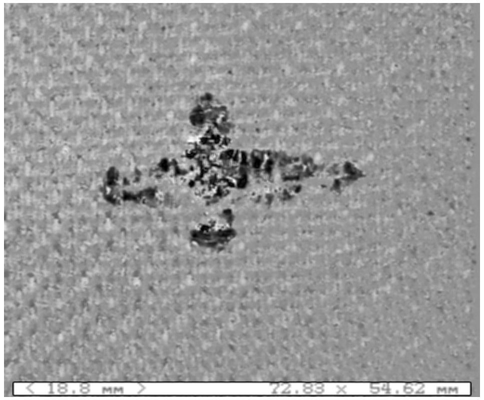

C-SCAN ultrasound image

CFRP panel after 20 Joule impact

Aircraft ultrasonic inspection (Composites World)

Current NDE Methods

Sandia National Laboratories

Non-Destructive Evaluation

Radiographic Evaluation
- X-Ray Computed Tomography
- X-Ray Radiography
- Neutron Radiography

Acoustic Evaluation
- Acoustic Emission
- Ultrasonic Scanning (A,B,C-Scans)
- Phased Array Ultrasonics

Thermographic Evaluation
- Passive Thermography
- Active Thermography (Flash)
- Pulsed Eddy Current Thermography
- Vibro-Thermography

Electro-Magnetic Evaluation
- Eddy-Current Evaluation
- Nuclear Magnetic Resonance

Scope of This Work

- Low velocity impact
  - CFRP panel
    - $[0/90]_9$
    - 100 mm × 150 mm
  - Drop-weight impact events
    - Subjected to 10, 20, 40, 60, and 80 J
    - 1.5″ diameter hemispherical tup
    - Fixed impactor weight
- NDE methods
  - X-Ray computed tomography
  - Active thermography (Flash)
  - Vibro-thermography
  - Ultrasonic C-scan
  - Electrical impedance tomography (EIT)

X-Ray Computed Tomography

- Hard tomographic method
  - Straight imaging path
    - Opposing x-ray source and detector
  - High resolution
    - Micron resolution
    - ~37 min acquisition time
  - High price
    - ~$100,000+
  - Computationally intensive reconstruction
- Experimental Setup
  - 130 kVp x-ray source (Phillips)
    - ~13 μm focal point
  - Varian 2520V amorphous Si detectors
    - CsI scintillator
    - 127 μm pitch

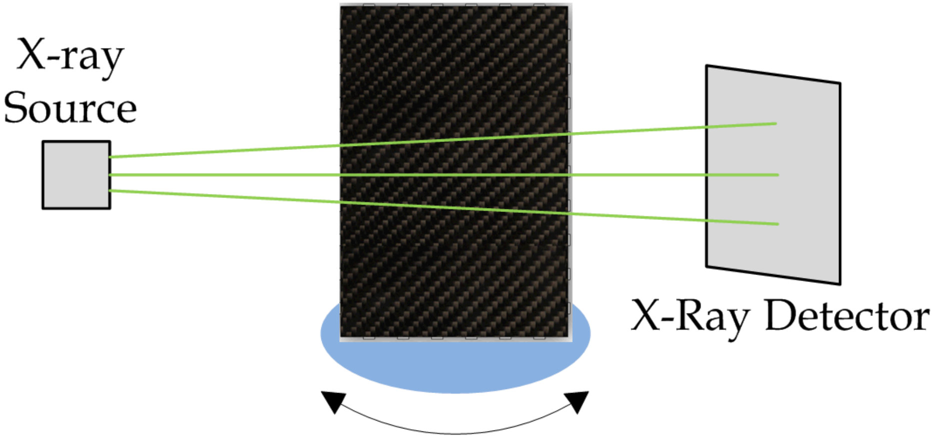

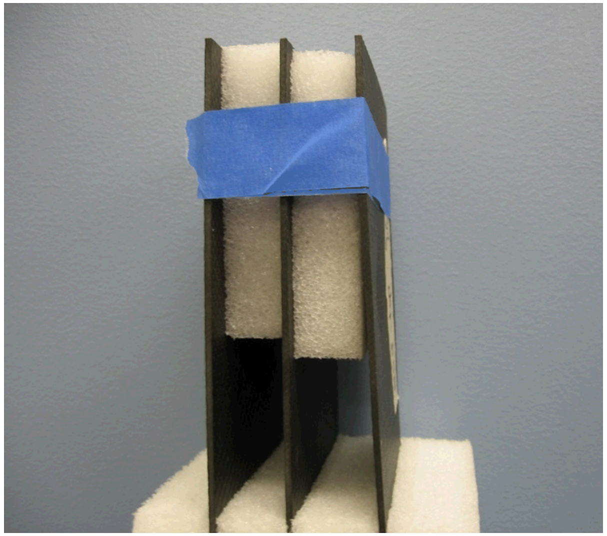

X-Ray CT Results

- Carbon fibers easily visible
  - X-Ray adsorption of carbon
  - Fiber bundles discernible
  - Fiber breakage
    - Bundles, not single fibers
  - Delamination
    - Fiber displacement
- Epoxy not visible
  - Extent of matrix damage
- Pros:
  - High-resolution imaging
  - Full reconstruction of part
- Cons:
  - Not sensitive to interfaces
  - Expensive

See other power point for video

80 J Impact Specimen

10 J Impact Specimen

Flash Thermography

- Transient thermal imaging
  - Subsurface defects detected
    - Thermal diffusivity mismatch
  - Epoxy/Air interface easily visible
    - Delamination
- FLASH Thermal Wave System
  - Flash lamps
  - Galileo IR camera
    - 60 frames/s
    - 256 x 256 pixels
  - Measurement time: < 1 min

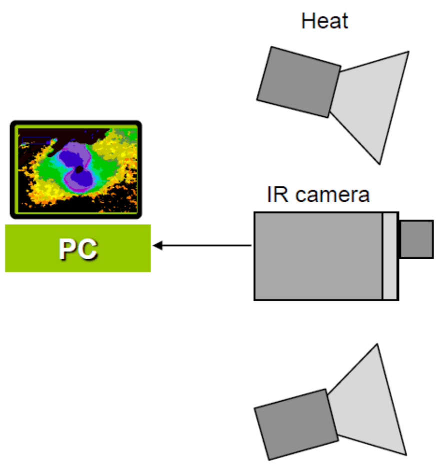

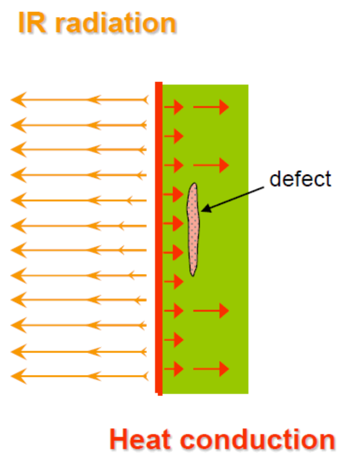

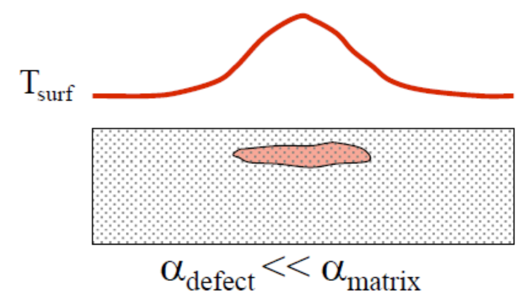

Surface temperature distribution

Excite Surface Layer → Probe Internal Structure → Measure Surface ΔT → Process

(Thermal Wave Imaging)

Flash Thermography Results

- Discontinuities visible
  - Delaminations
  - Composite cracking
  - Subsurface discontinuities
    - Deeper discontinuities appear later
- Pros
  - Discontinuities are prominent
    - Damage indicated
    - Perfect for delamination
- Cons
  - Lower resolution
  - Lower sensitivity
    - Cracks parallel to pulse
    - Damage can mask underlying damage

See other power point for video

80 J Impact Specimen

10 J Impact Specimen

Vibro-Thermography

- Imaging technique
  - Ultrasonic actuation
  - Thermal imaging
  - Waves generate heat at interfaces (damage) within specimens
- Experimental Setup
  - 1 kW, 20 kHz ultrasonic source
    - 0.2 s burst
  - High speed thermal imager
  - Images taken:
    - Start ultrasonic actuation
    - End ultrasonic actuation
    - After ultrasonic actuation
  - Measurement time: < 1 min
  - Only 10 J specimens imaged

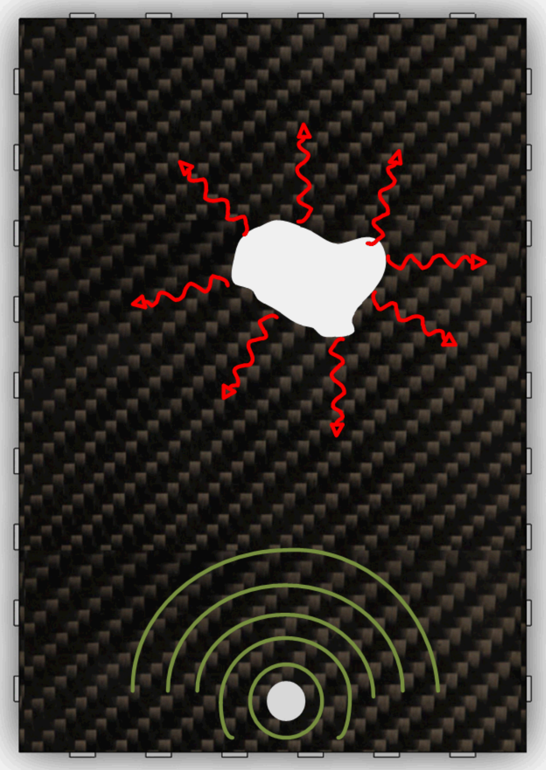

Vibro-Thermography Results

- Discontinuities radiant heat
  - Matrix cracking
  - Fiber breakage
- Beginning of excitation
  - Surface waves heating surface damage
- After excitation
  - Heat generation is at a maximum
  - Indicative of deeper located damage radiating outward
    - Typical of composites
- Pros:
  - Discontinuities visible
- Cons:
  - Lower resolution
  - Not as sensitive to delamination

After ultrasonic actuation

Ultrasonic C-Scan

- Pulse-echo imaging
  - A-scan
    - Reflected energy in time
  - B-scan
    - Through thickness scan
  - C-scan
    - Rastered, lines of pixels
  - Effective at imaging interfaces
    - Dissimilar acoustic impedances
    - Attenuation limits depth of scan
- Experimental Setup
  - Focused Transducer
    - 5 MHz
    - 1.5" focal length
  - Scanning Time: ~5-60 min
    - Resolution dependent

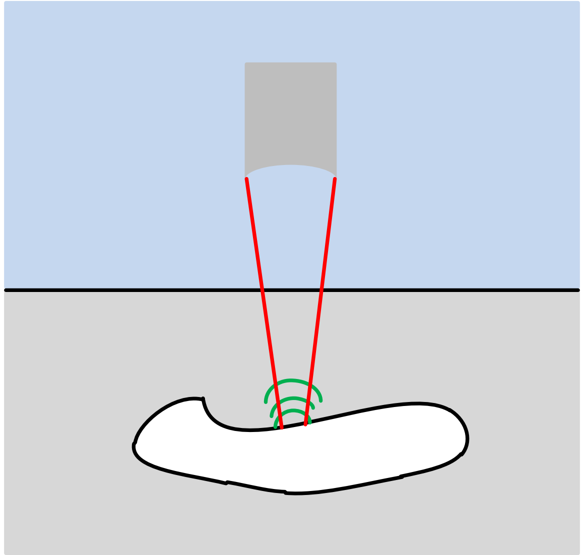

Focused imaging schematic

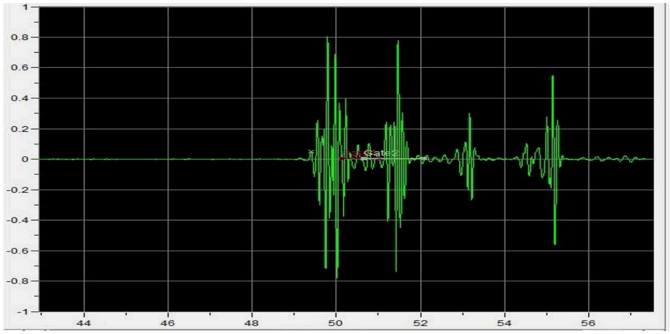

Example A-scan

Ultrasonic C-Scan Results

- Sensitive to interfaces
  - Changes in acoustic impedance
    - Delaminations
    - Fiber bundle-matrix interface
    - Some cracks transverse to waves
- Pros:
  - Sensitivities:
    - Delamination
    - Geometry changes
  - Hand-held compatible
- Cons:
  - Insensitive to fiber breakage
    - Uniaxial tensile tests
  - Lower sensitivity to over-lapping damage

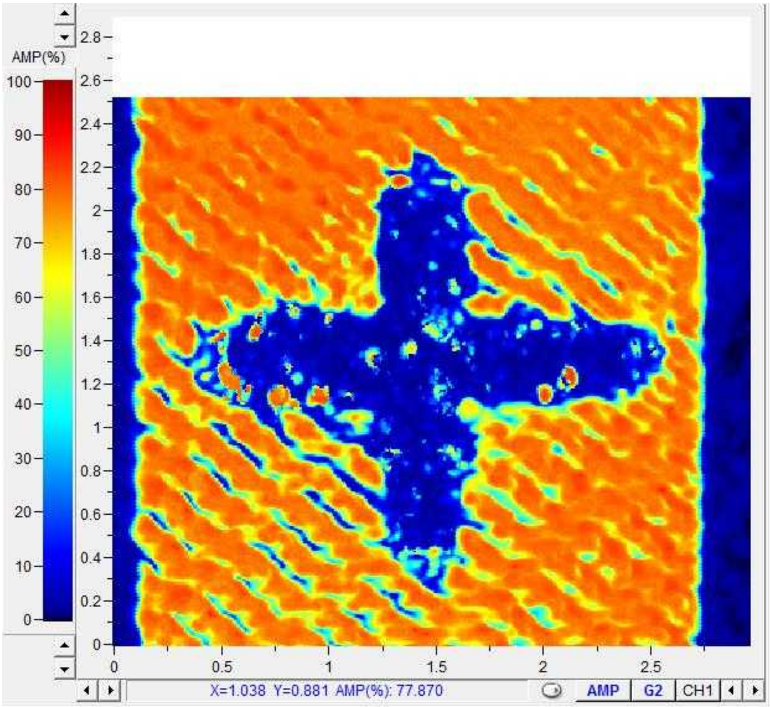

C-Scan of 80 J impact specimen

SHM Design Considerations

Current NDE limitations:

- Labor intensive
- Expensive equipment
- Structures must come out of service
- Experience technician required to interpret results

Boeing 787 (Boeing)

Successful SHM systems:

1. Directly detect and measure damage
2. Determine the damage location
3. Ascertain the size of the damage
4. Quantify the severity of the damage
5. Achieve multi-modal sensing capabilities (i.e., delamination, cracking, and chemical penetration)

Golden Gate Bridge (Wikipedia)

Fiber Optic Sensors

- Light-based method
  - Reflection/refraction of light used for sensing
- Sensors
  - Fiber bragg gratings
    - Strain/temperature
  - Brouillon sensors
    - Strain/temperature
  - Plain
    - Crack detection
- Benefits
  - Embeddable
  - Radiation insensitive
  - High density of sensors along one fiber

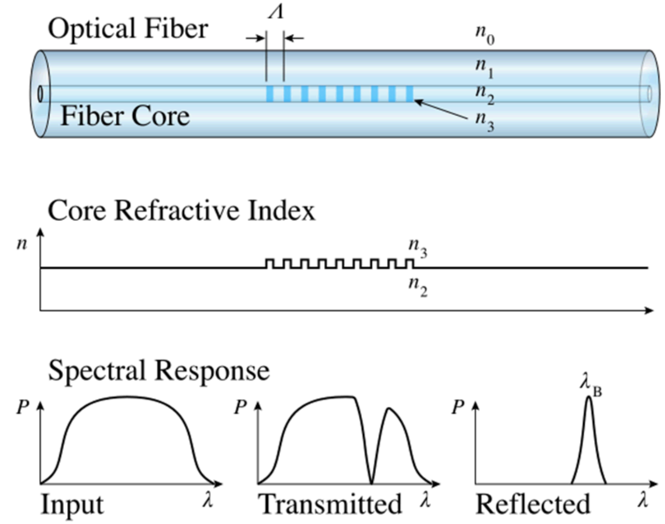

Explanation of a fiber bragg grating sensor (Wikipedia)

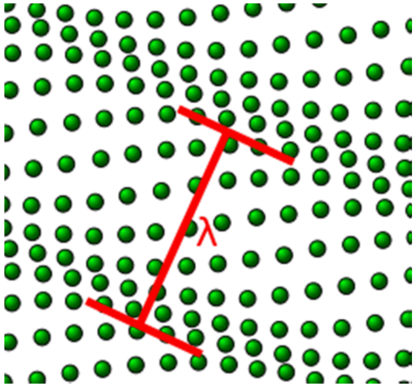

Density/refractive index changes that cause Brillouin scattering (Wikipedia)

Embedded Fiber Optics

- Layup composite with embedded optical fibers
- Positives
  - Sense damage/strain internal to composite
  - Resin cure monitoring
    - Temperature distribution
    - Residual stress field from cure
- Negatives
  - Fiber diameter <100 microns leads to decrease in fatigue performance
  - High stress concentration where fiber enters composite
    - Leads to easily fiber fracture

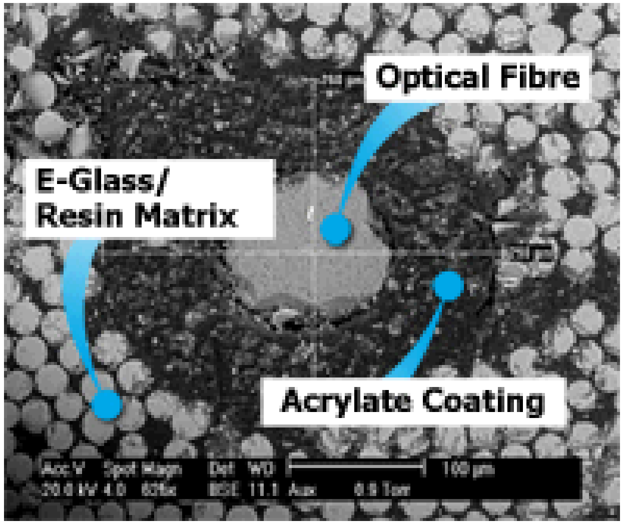

SEM image of embedded optical fiber in GFRP composite (Epsilon Optics)

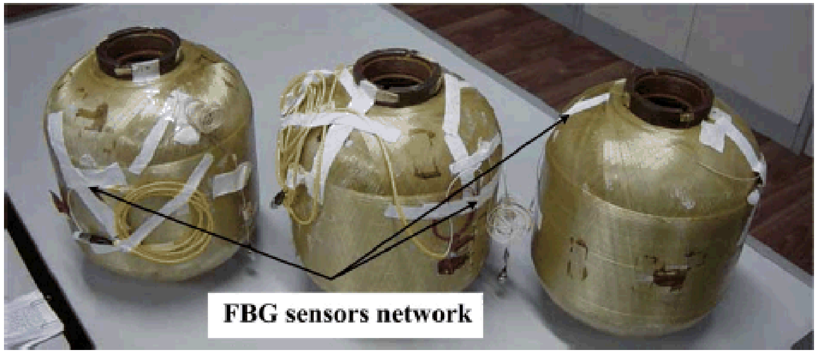

FBG optical fibers embedded in rocket motor GFRP structure (2008 X. Chang et al.)

Acoustic Emission

- Approach
  - Piezoelectric sensor applied/embedded to composite
  - Monitor for emission of sound from damage event
  - Characteristic of emission used to determine damage type
- Positives
  - Can localize and characterize damage event
- Negatives
  - Constant monitoring at high data rate to detect damage events
  - Equipment can be bulky and expensive
    - Getting a lot better

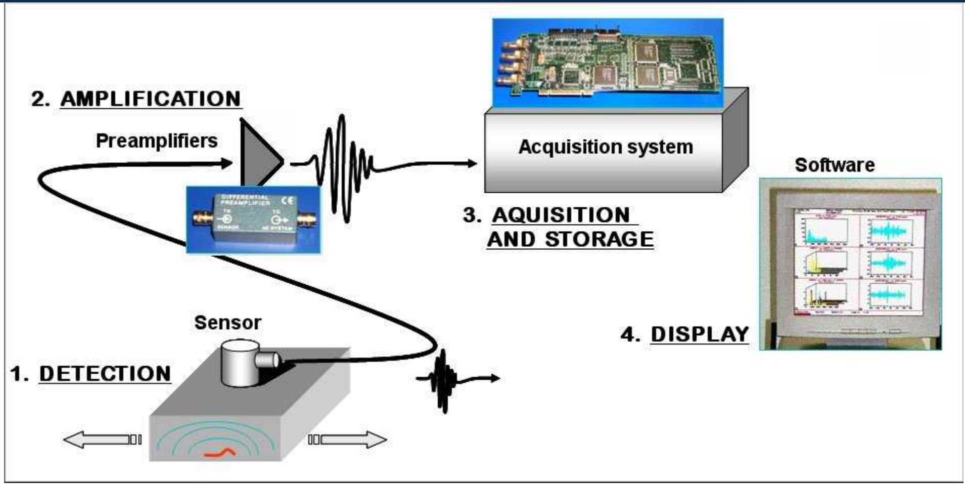

SEM image of embedded optical fiber in GFRP composite (Mistras Group)

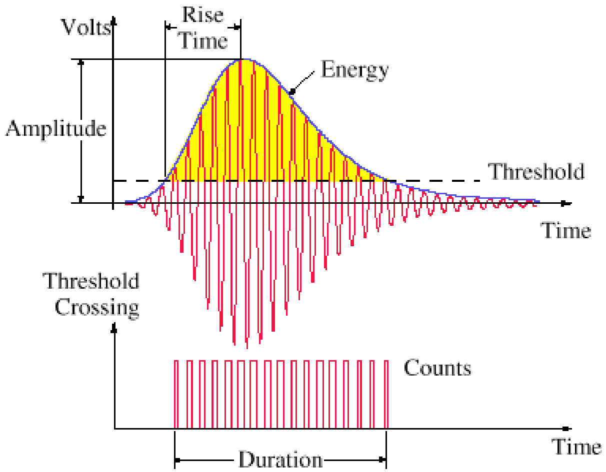

SEM image of embedded optical fiber in GFRP composite (TMS)

Ultrasonic-based sensing

- Approach
  - Propagate a stress wave across the structure using piezoelectric
  - Wait for response at same or other sensor
  - Analyze for spatial and damage characteristics
- Positives
  - Rapidly maturing field
  - Sensitive to many damage modes
  - Can localize damage
- Negatives
  - Data acquisition and amplifiers can be bulky
    - Recent efforts have reduced hardware significantly

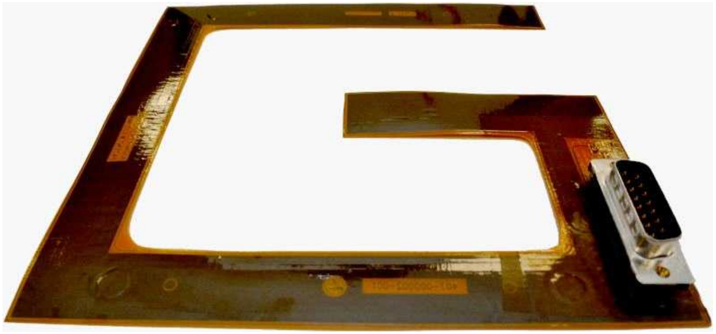

Acellent's Smart Layer ultrasonic sensors (Acellent Technologies)

Metis Disk ultrasonic-based sensors (Metis Design)

Embedded Sensing via CNT Thin Films

PART I

Development of carbon nanotube-based nanocomposites for multi-modal sensing

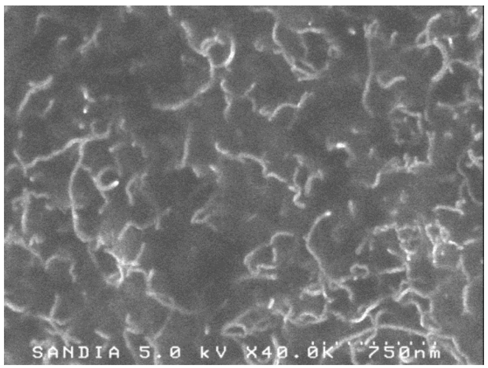

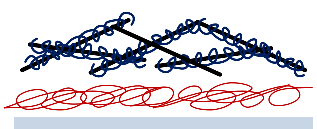

1. Harness unique material properties of carbon nanotubes

2. Layer-by-layer "bottom-up" thin film multi-modal sensor design

PART II

Embedded nanocomposite strain sensors for glass fiber-reinforced polymer composites

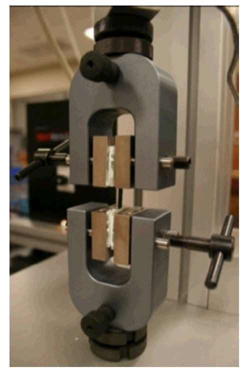

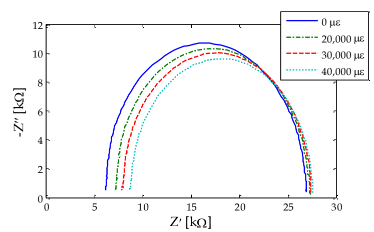

3. Deposited thin films on FRP for strain sensing

4. MWNT-latex multi-modal sensor via spray deposition

PART III

From point-sensing to distributed sensing using sensing skins

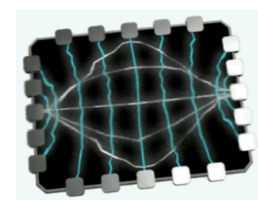

5. Electrical impedance tomography for spatial conductivity mapping

6. Distributed spatial damage sensing based on sensing skins

Carbon Nanotubes

- Multi-walled carbon nanotubes (MWNT):
  - Rolled concentric cylindrical structures constructed of graphene sheets
  - Diameter: 6 ~ 100 nm
  - High-aspect ratios: ~10^3 to 10^7
  - Metallic conductivity
  - Five times stiffer and ten times stronger than steel

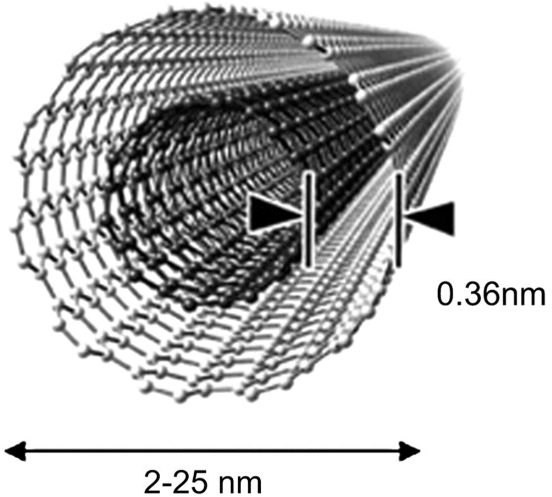

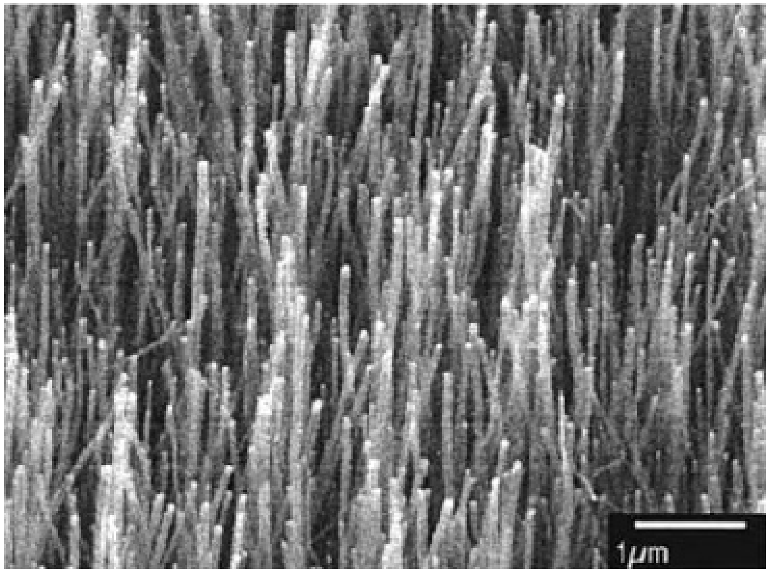

Aligned carbon nanotube forest
Thostenson, et al. (2001)

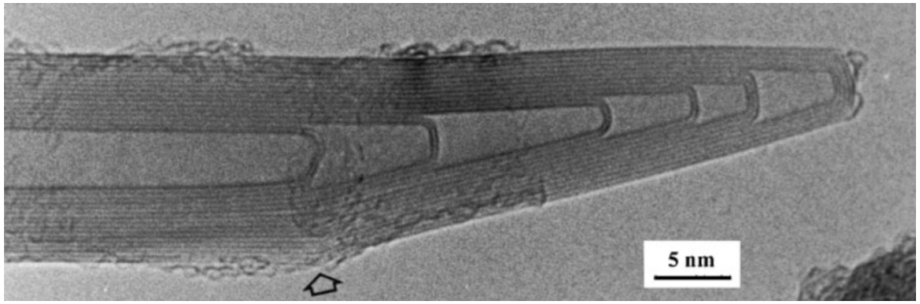

TEM imagery of an end cap of a MWNT
Harris (2004)

Layer-by-Layer (LbL) Method

- Sequential assembly of oppositely-charged nanomaterials onto a charged substrate
  - Bottom-up fabrication methodology
  - Incorporation of a wide variety of nanomaterials
  - 2.5-dimensional nano-structuring to design multifunctional composites
- Excellent physical, mechanical, and electrical properties:
  - Physical: homogeneous percolated nano-scale morphology
  - Mechanical: high strength, stiffness, and ductility

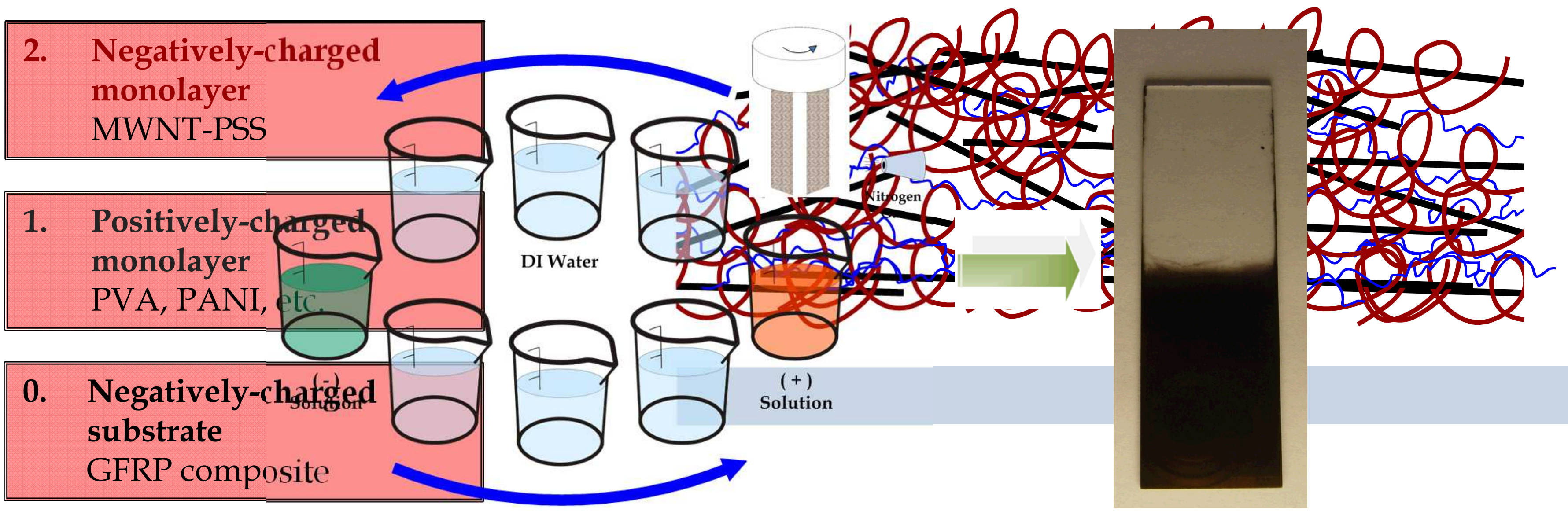

Nanocomposite Morphology

- Mechanical strength and electrical conductivity/sensing derived from percolated thin film morphology
  - Homogeneous composite with similar properties across entire film
  - Scanning electron microscopy (SEM) imagery to evaluate percolation and uniformity

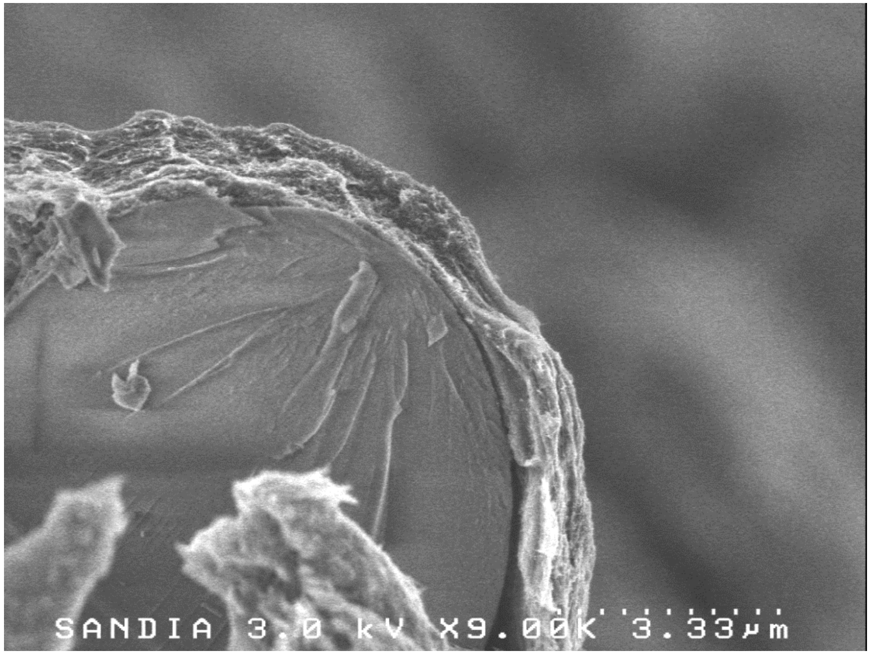

Scanning electron microscopic (SEM) cross-section view of a [MWNT-PSS/PVA]$_{150}$ thin film on GFRP

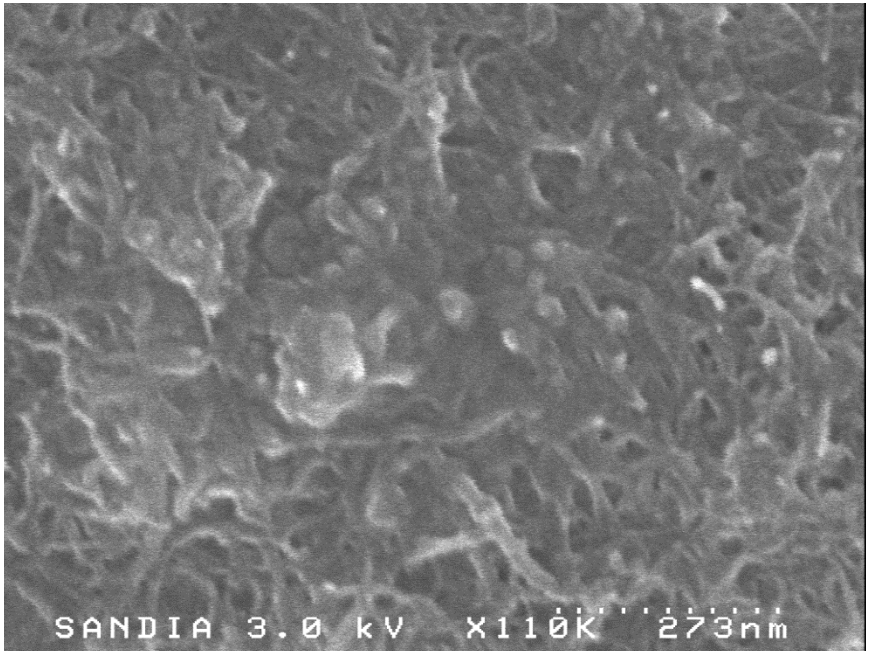

Surface SEM image of a [MWNT-PSS/PVA]$_{100}$ thin film

Presentation Outline

PART I

Development of carbon nanotube-based nanocomposites for multi-modal sensing

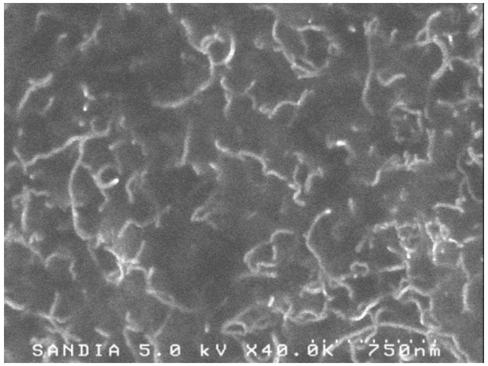

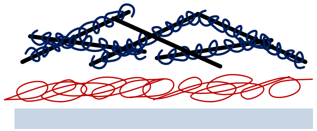

1. Harness unique material properties of carbon nanotubes

2. Layer-by-layer "bottom-up" thin film multi-modal sensor design

PART II

Embedded nanocomposite strain sensors for glass fiber-reinforced polymer composites

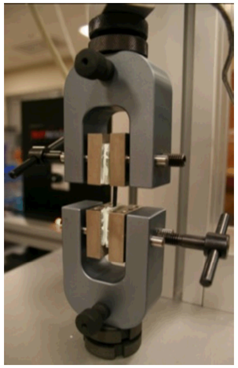

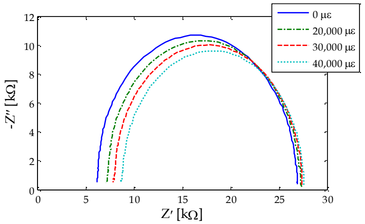

3. Deposited thin films on FRP for strain sensing

4. MWNT-latex multi-modal sensor via spray deposition

PART III

From point-sensing to distributed sensing using sensing skins

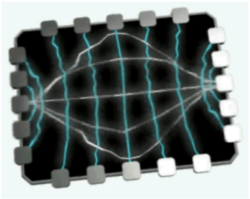

5. Electrical impedance tomography for spatial conductivity mapping

6. Distributed spatial damage sensing based on sensing skins

Strain Sensitivity Validation

- Objective:
  - Validate thin film electromechanical performance deposited on GFRP
- Specimen preparation:
  - Attach two conductive electrodes and composite tabs
- Nanocomposite electromechanical performance characterization:
  - Apply monotonic and dynamic uni-axial tensile loading to specimens

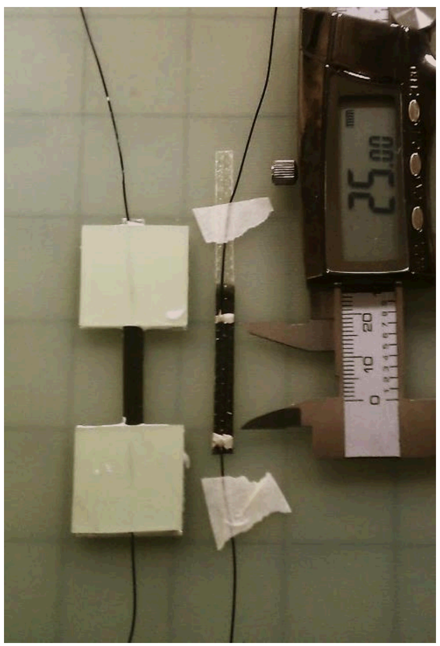

Fiber-coated specimen

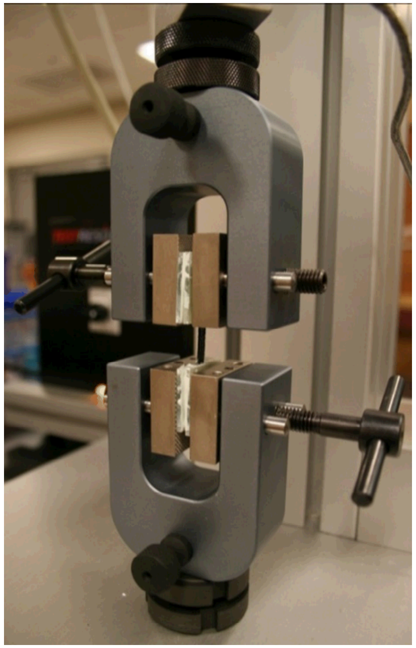

Thin film mounted in load frame

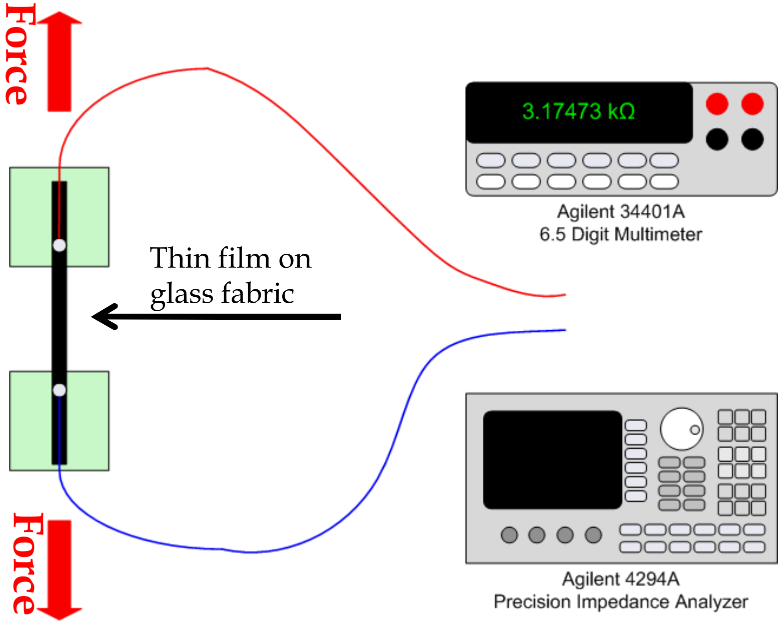

Time- and frequency-domain strain sensing

Sandia National Laboratories

- Electrical impedance spectroscopy:
  - Provides greater insight as compared to bulk resistivity measurements
  - Measurement of complex electrical impedance across spectrum of frequencies (40 Hz – 110 MHz)

$$Z(\omega) = \frac{V(j\omega)}{I(j\omega)} = |Z(\omega)| \angle \phi(\omega) = Z'(\omega) + jZ''(\omega)$$

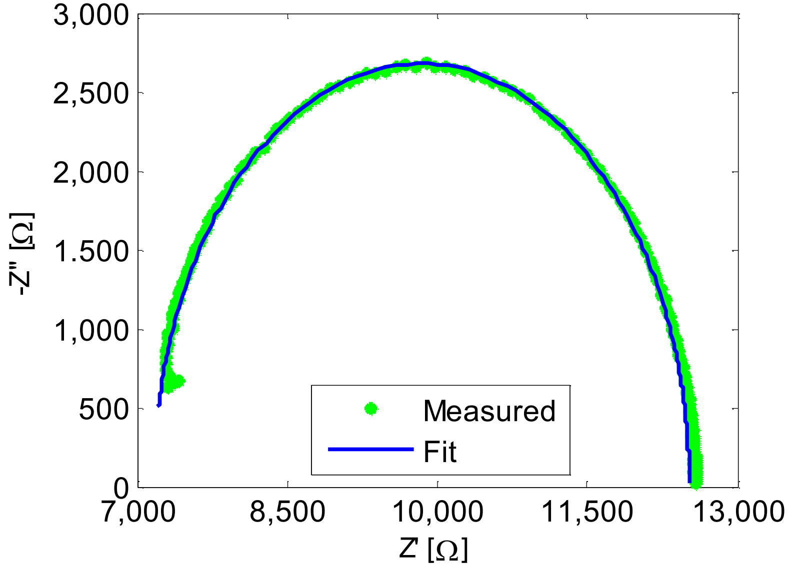

  - Physically-based equivalent circuits are used to fit to the impedance data

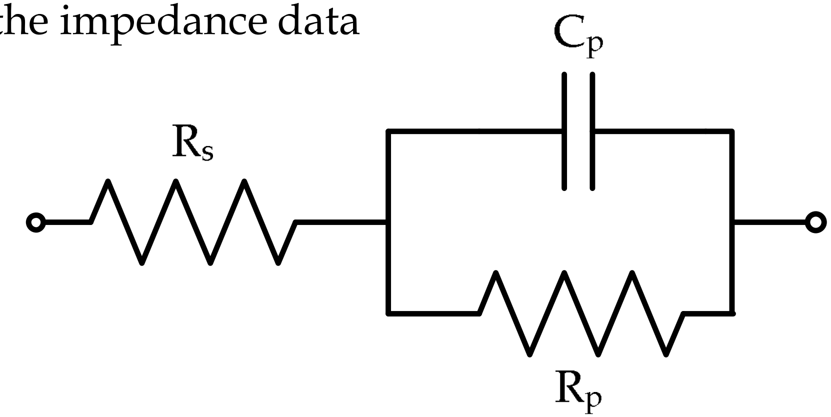

Proposed equivalent circuit model for LbL thin films

Monotonic Sensor Characterization

- Load frame applies stepped-tensile displacement profile:
  - Monotonic increasing strain to failure
  - Capture full sensors response
- Equivalent circuit model-updating:
  - Fitting with nonlinear least squares
  - Extract fitted circuit parameters as a function of applied strain
- Bi-functional strain sensitivity:
  - Low strain region:
    - Linear response (elastic)
  - High strain region:
    - Quadratic Response
    - Damage to GFRP/thin film

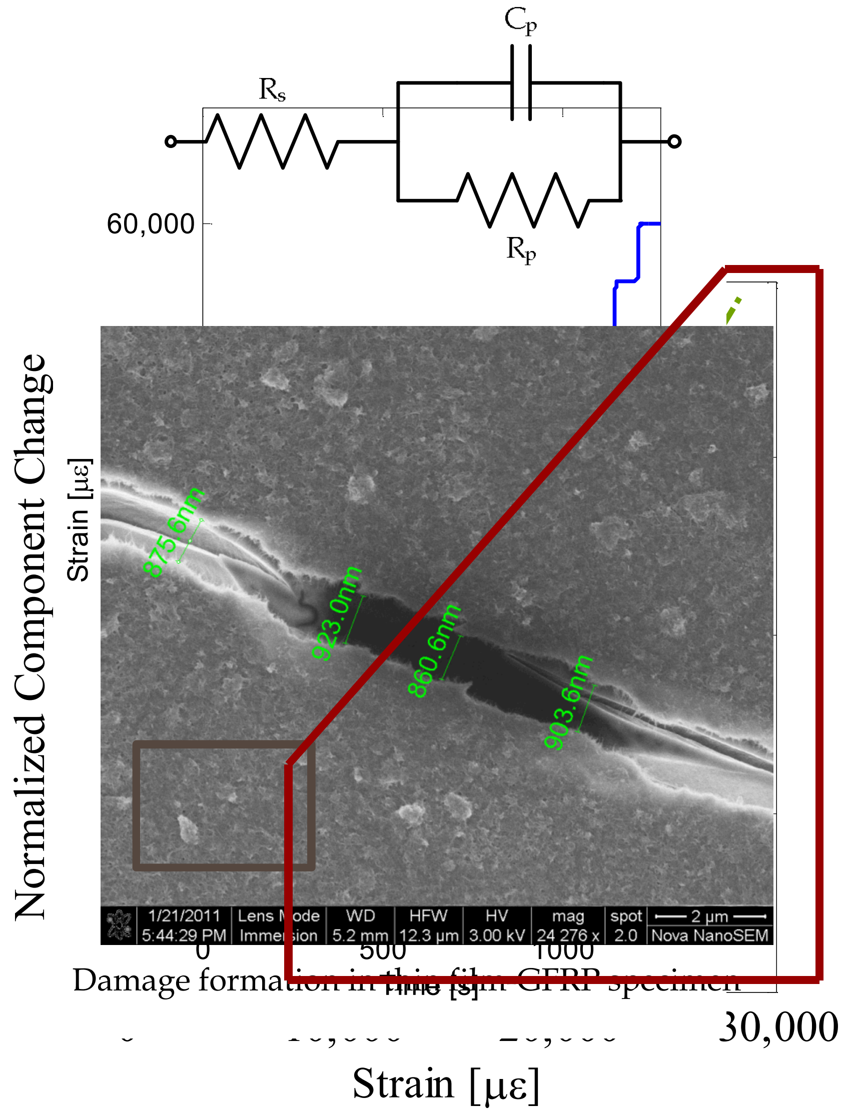

Dynamic Sensor Characterization

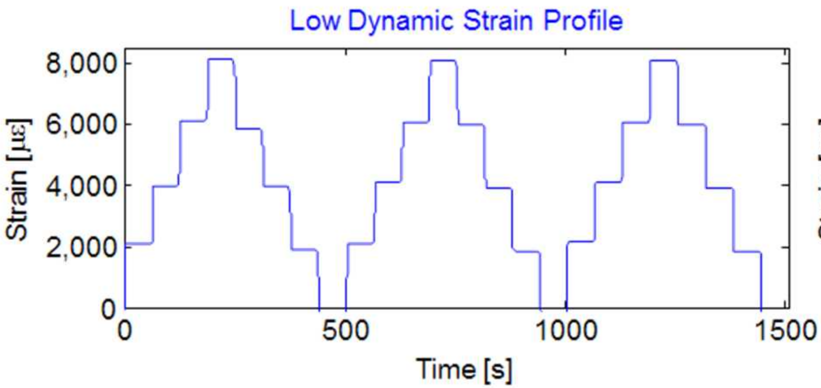

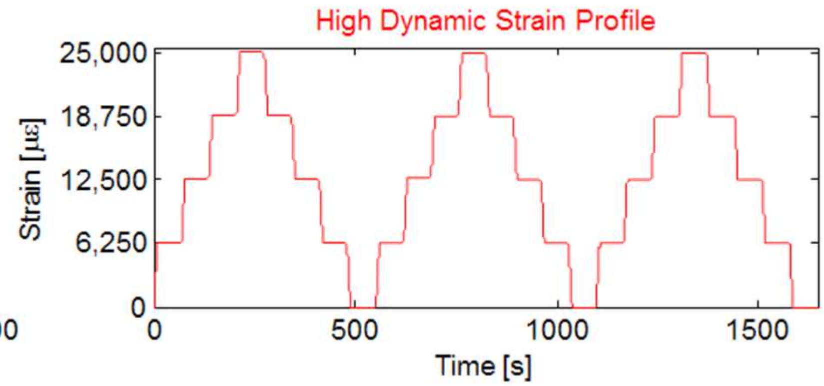

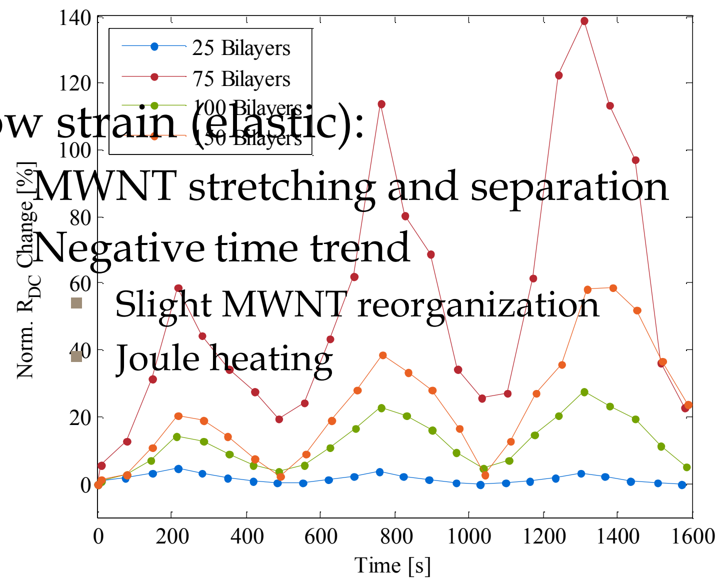

- Low strain (elastic):
  - MWNT stretching and separation
  - Negative time trend
    - Slight MWNT reorganization
    - Joule heating

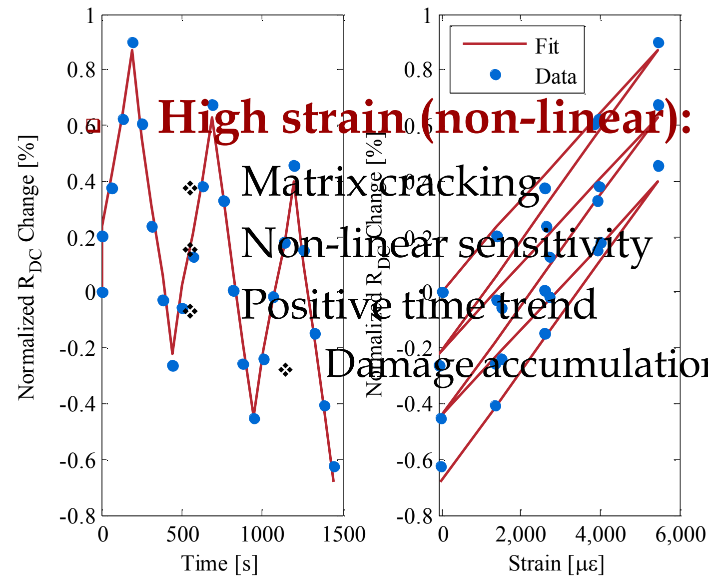

- **High strain (non-linear):**
  - Matrix cracking
  - Non-linear sensitivity
  - Positive time trend
    - Damage accumulation

Preliminary Results

Sandia National Laboratories

- Application of a strain sensitive carbon nanotube thin film:
  - Layer-by-layer deposition process
  - Direct deposition on GFRP
  - Demonstrated piezoresistivity
- Bi-function strain sensitivity:
  - Time and frequency-domain characterization
  - Demonstrated in monotonic and dynamic loading
  - Low strain region:
    - Linear strain sensitivity
  - High strain region:
    - Quadratic sensitivity
    - Damage accumulation
- Deposition limitations:
  - Substrates required to be less than a few square inches in size

Sprayable MWNT-Latex Thin Film

- Rapid large-scale deposition
  - Required for mass deployment of methodology

- MWNT-PSS/Latex paint formulation
  - Collaborated to improve initial Sandia formulation
  - Sub-micron PVDF creates mold for MWNT organization
  - Off-the-shelf deposition method

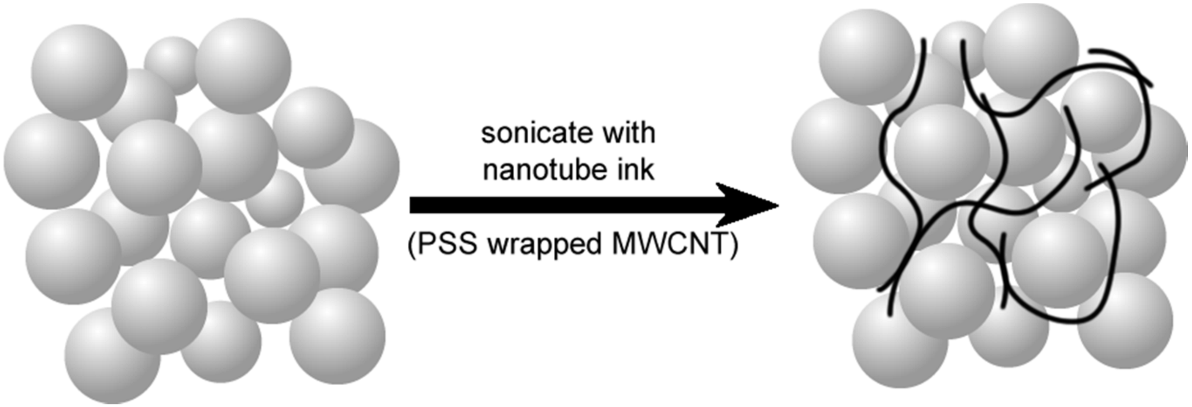

Kynar Aquatec™ latex solution (avg. particle size 150nm)

Forms segregated MWCNT network

MWNT-Latex Morphology

- Creation of MWNT networks:
  - Electrical percolation above 1 wt% MWNTs

- Fiber-reinforced polymer deployment:
  - Surface applied to post-cured composites
  - Applied to fiber weaves for embedded sensing

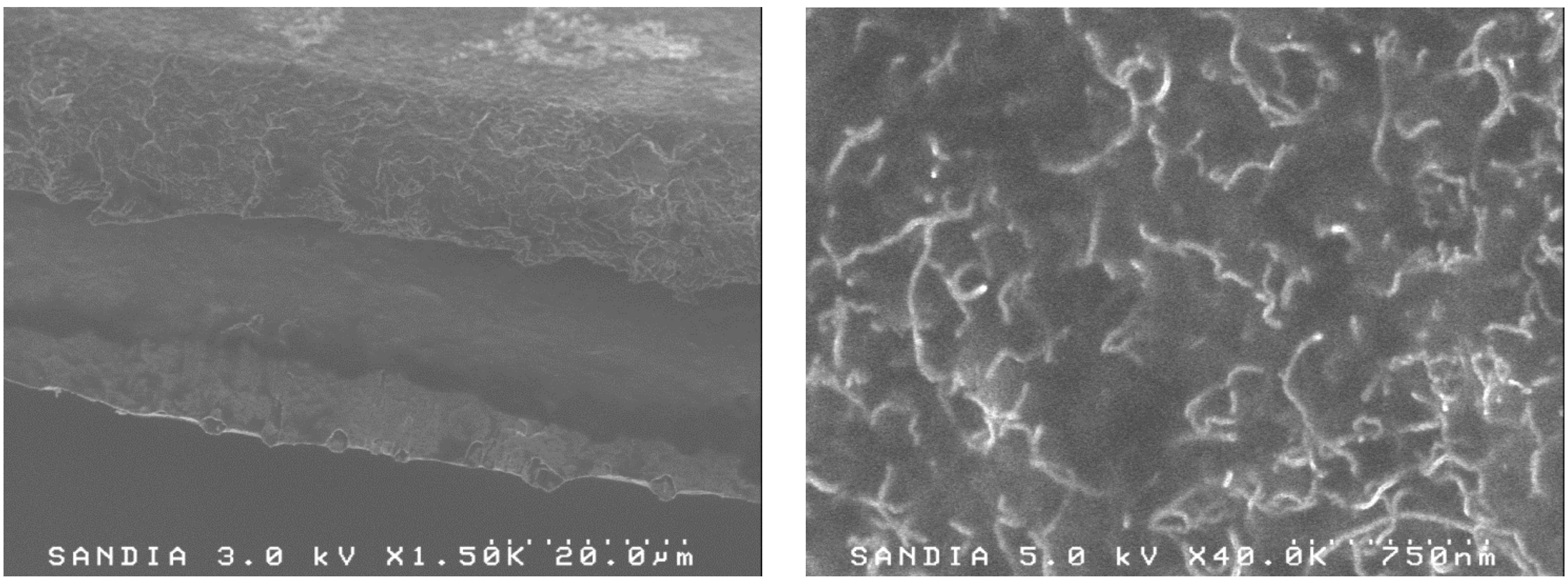

Cross-section and MWNT network SEM images of 3wt% MWNT-Latex film

MWNT-Latex Characterization

- Electromechanical characteristics:
  - Quasi-static testing
    - Nearly same sensitivity as LbL
  - Bi-functional strain response
    - Linear
    - Quadratic
      - Cracking of film
- Thermo-resistance coupling:
  - -50° C to 80° C over 2 hours
  - 2 hour holds
  - Inversely linear relationship
  - Non-linear response @ -30° C
    - ~ T_g of PVDF
    - Restructuring of MWNTs

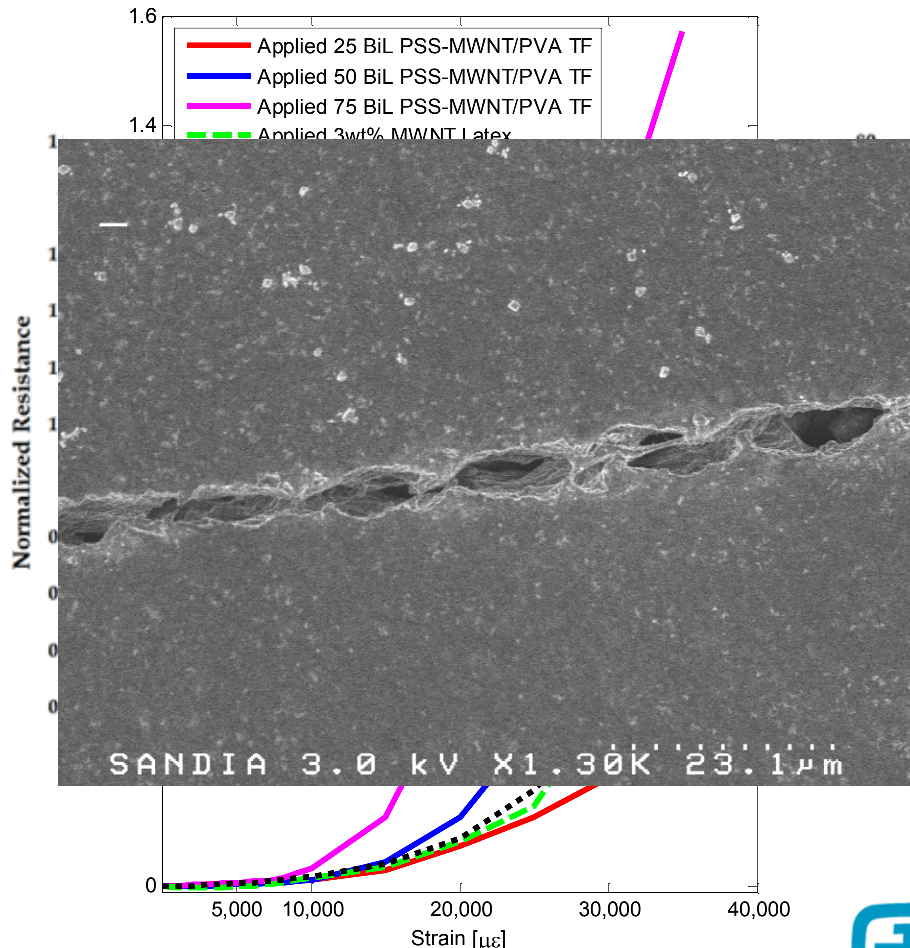

Presentation Outline

PART I

Development of carbon nanotube-based nanocomposites for multi-modal sensing

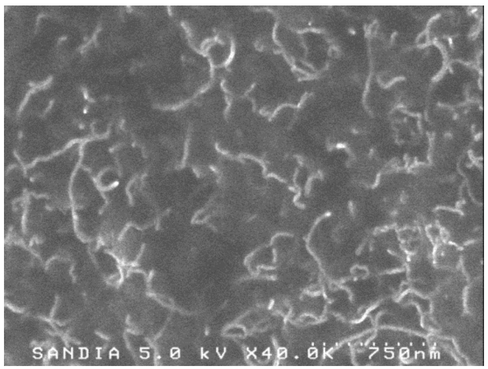

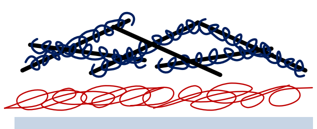

1. Harness unique material properties of carbon nanotubes

2. Layer-by-layer "bottom-up" thin film multi-modal sensor design

PART II

Embedded nanocomposite strain sensors for glass fiber-reinforced polymer composites

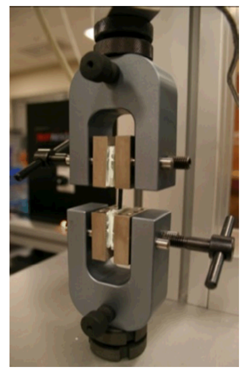

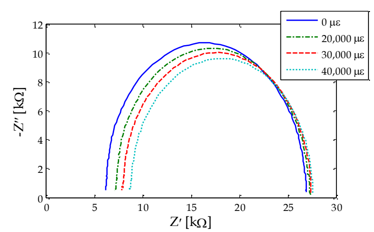

3. Deposited thin films on FRP for strain sensing

4. MWNT-latex multi-modal sensor via spray deposition

PART III

From point-sensing to distributed sensing using sensing skins

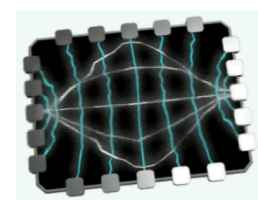

5. Electrical impedance tomography for spatial conductivity mapping

6. Distributed spatial damage sensing based on sensing skins

Spatially Distributed SHM Paradigm

- Current state-of-art in structural health monitoring:
  - Passive SHM using acoustic emissions
  - Active SHM using piezoelectric sensor/actuator pairs
- "Sensing skins" for spatial damage detection:
  - Objective is to identify the location and severity of damage
  - Monitor and detect damage over two- (or even three) dimensions
  - Direct damage detection

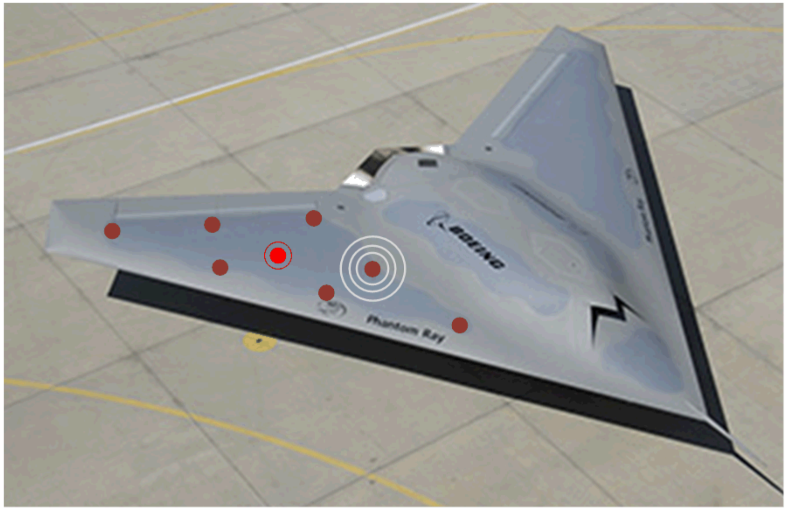

(Boeing)

(Boeing)

Electrical Impedance Tomography

- Overview of spatial conductivity mapping
  - Since film impedance calibrated to strain, conductivity maps can correspond to 2-D strain distribution maps

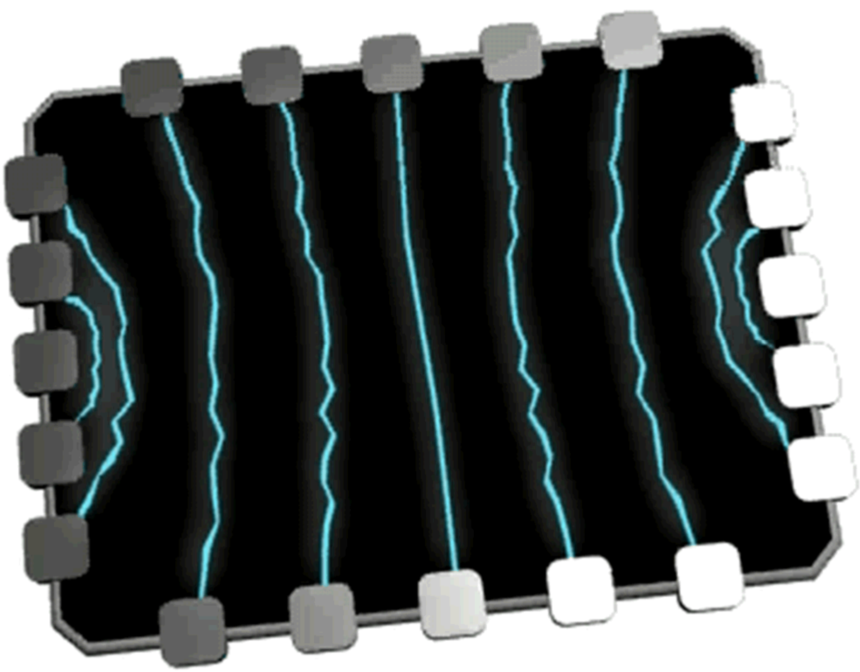

Typical EIT Reconstruction

- Laplace's equation:
  - $\nabla \cdot (\sigma \nabla \phi) = 0$, where σ can vary by orders of magnitude
  - Governs potential and conductivity relationship
- Forward problem: conductivity known, solve voltage
- Inverse problem: voltage known, solve conductivity

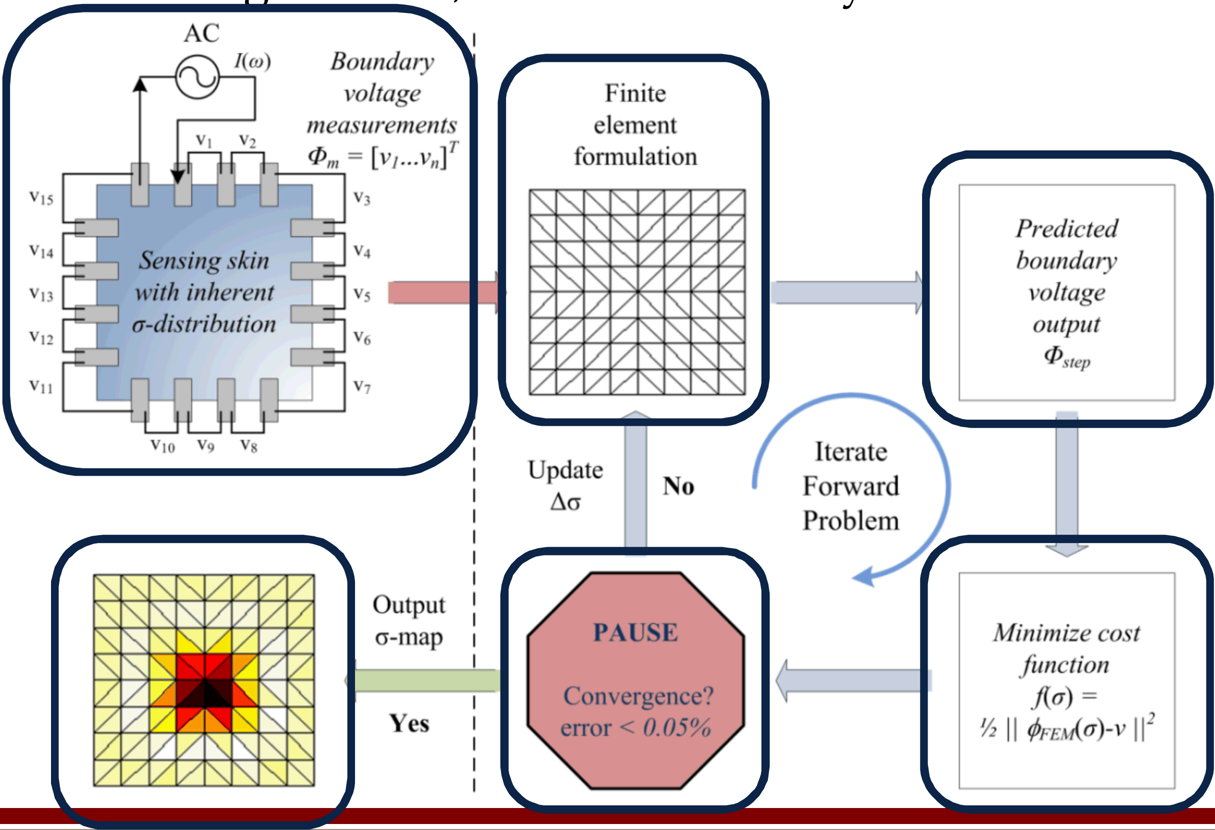

Linear EIT Reconstruction

- Reconstructs small σ changes:
  - Typically difference imaging
    - $\sigma_1 - \sigma_2 << \sigma_2$
- Maximum a posteriori (MAP):
  - H: sensitivity matrix
    $$H(\sigma_{bkgd})_{ij} = \frac{\partial V_i}{\partial \sigma_j}$$
  - Regularization hyperparameter: λ
    - Noise figure
    $$NF(\lambda) = \frac{SNR_{in}}{SNR_{out}} \approx 1$$
    - Use representative σ distribution
  - W: Noise model
  - R: Regularization matrix
- Advantages:
  - Can pre-calculate H
  - Many damage modes lead to small changes in σ

$$\frac{\Delta\sigma}{\sigma_0} = \left(\underline{H}^T W \underline{H} + \underline{\lambda} R\right)^{-1} \left(\underline{H}^T W\right) \frac{\Delta V}{V_0}$$

$$\frac{\Delta\sigma}{\sigma_0} = B\Delta \frac{\Delta V}{V_0}$$

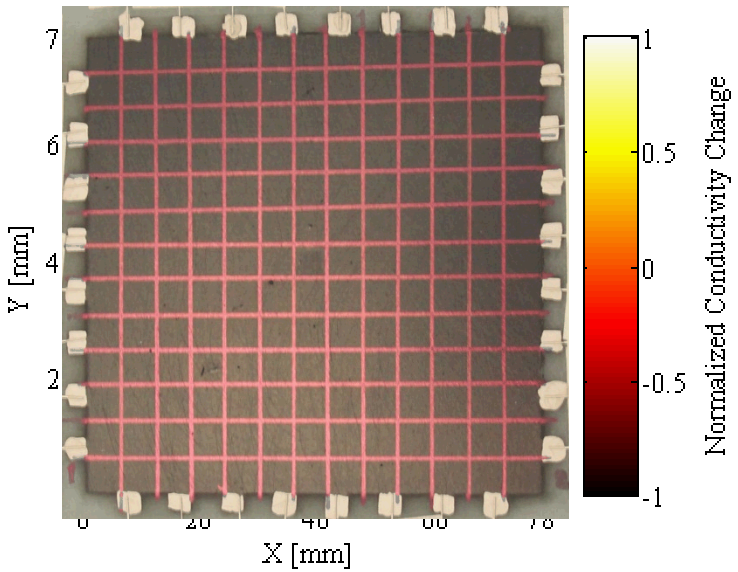

Validation EIT

- Applied sensing measurements
  - MWNT-Latex deposited upon cured GFRP composites
  - 78 mm x 78 mm sensing region
  - 8x8 electrodes scheme = 32 electrodes
    - 3 mm electrodes
    - 6 mm spacing
- Investigate stability and efficiency:
  - Computational demand
    - ~ 1 s reconstruction time
- Accuracy characterization:
  - Conductivity:
    - Point-to-point resistance map via 4-pt probe
  - Spatial feature ID sensing resolution
    - ~ 6 mm cross at center with -50% Δσ

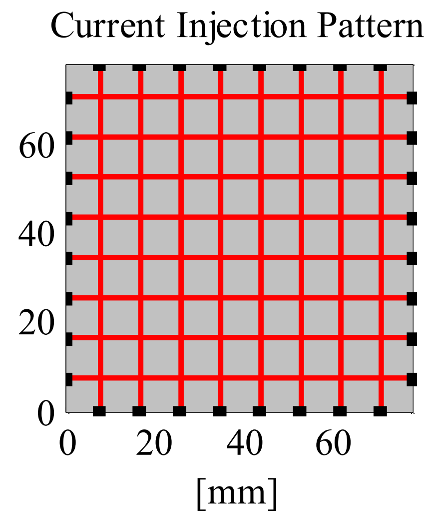

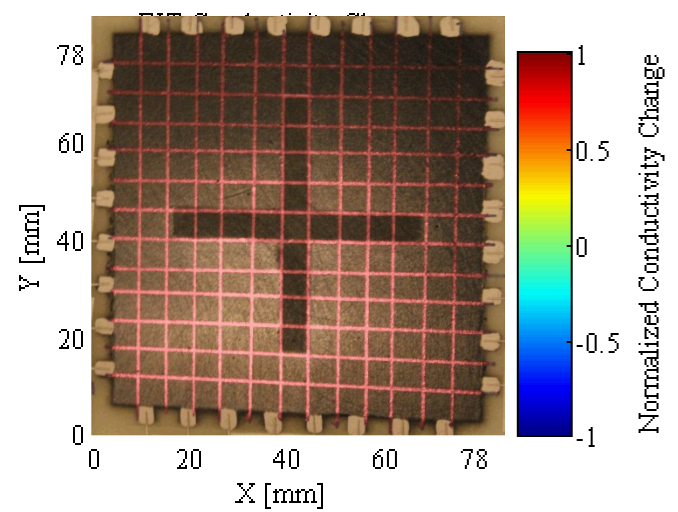

Spatial Strain Sensing

- 4-pt bending
  - **ASTM D7264**
  - MWNT-Latex on GFRP
  - Stepped displacement profile
  - Tensile/compressive strain
- Strain sensitivity
  - Nearly linear

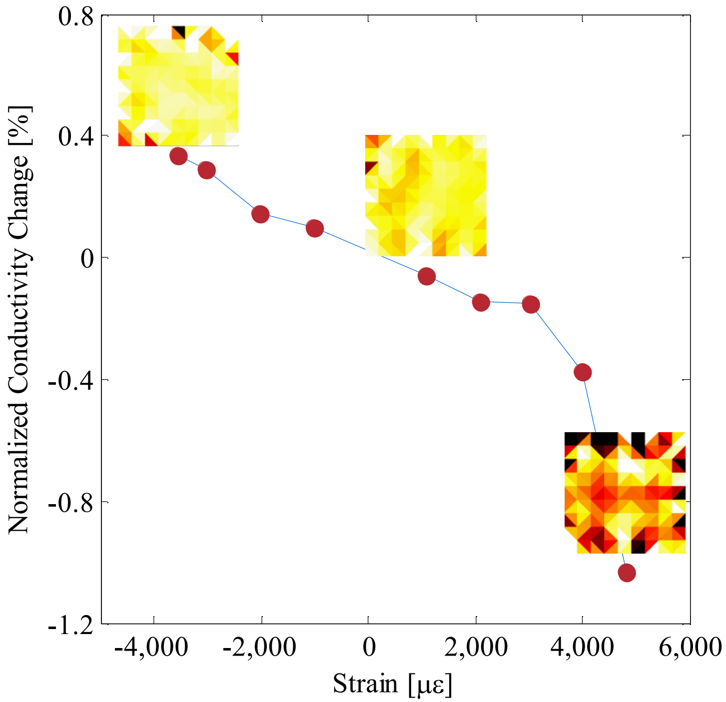

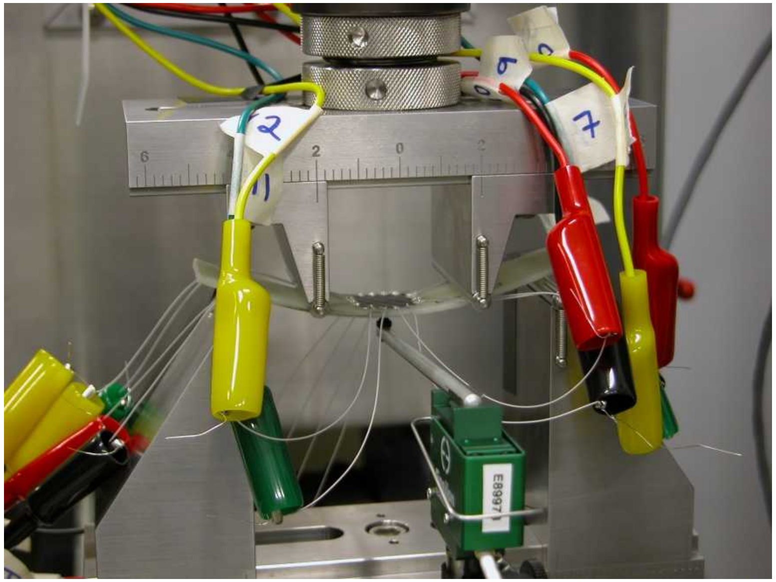

Embedded Spatial Sensing

- Embedded sensing architecture
  - MWNT-Latex on GF fiber weave
  - Embedded within epoxy matrix
- Specimens
  - $[0^\circ\ /+45^\circ\ /90^\circ\ /-45^\circ\ ]_{2s}$
  - Unidirectional GF
  - 150 mm x 100 mm
    - ASTM D7146 Standard
- Anisotropic EIT
  - Isotropic ▸ Anisotropic
  - Scalar ▸ Matrix: σ
  - $\sigma_{0^\circ} > \sigma_{90^\circ}$ by ~2:1
  - $$\nabla \cdot \left(\sigma \, \nabla \phi \right) = 0$$

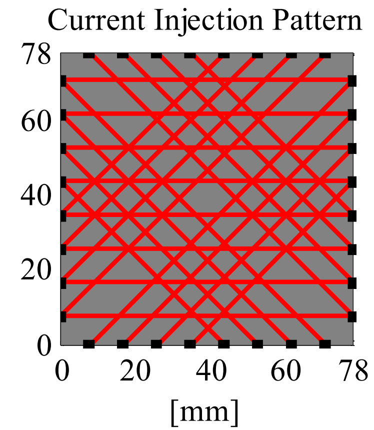

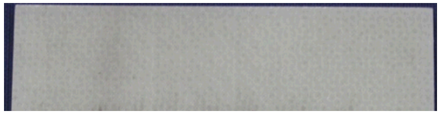

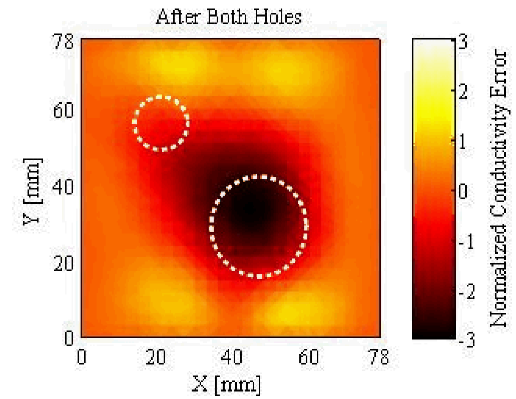

Embedded Spatial Sensitivity

- Embedded sensing validation:
  - Determine conductivity change sensitivity
  - Process:
    - Progressively larger drilled holes:
    - $^1/_{16}$″, $^1/_8$″, $^3/_{16}$″, $^1/_4$″, $^5/_{16}$″, $^3/_8$″, $^1/_2$″
  - Anisotropic EIT performed
    - Conductivity change from pristine sample

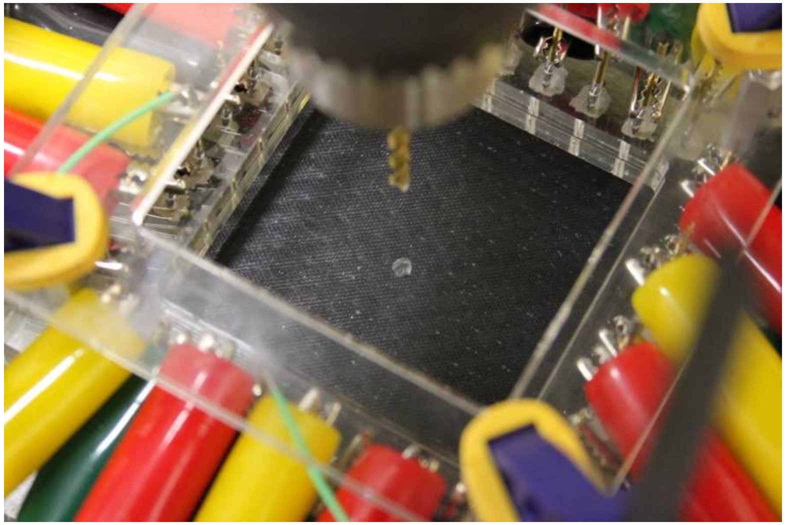

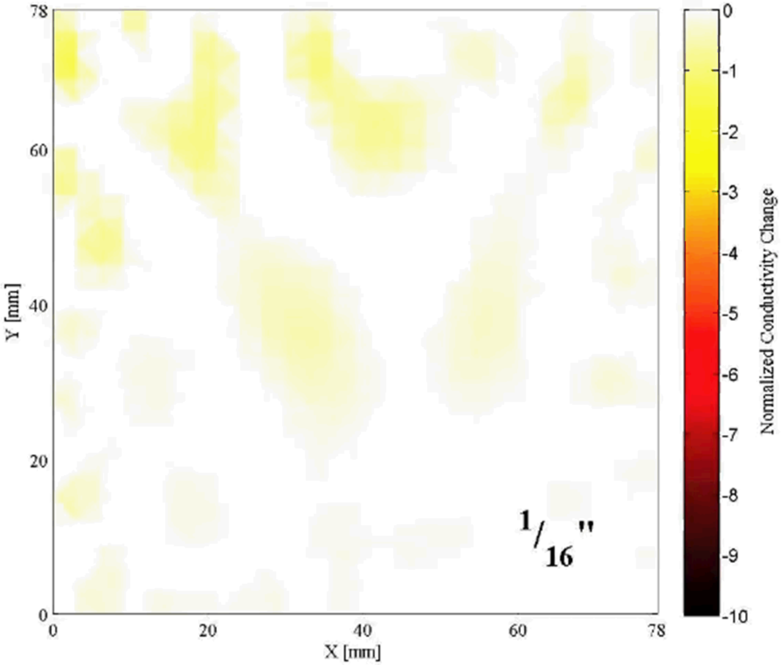

Impact Damage Detection

- Drop-weight impact tests
  - **ASTM D7146**
  - 78 mm by 78 mm sensing region
  - MWNT-latex on glass fiber weave
  - Impact energy: 20, 60, 100, 140 J
  - Before/after EIT measurements

- Verification:
  - Thermography
    - Matrix Cracking
    - Delamination
  - Photographic Imaging
    - Surface damage

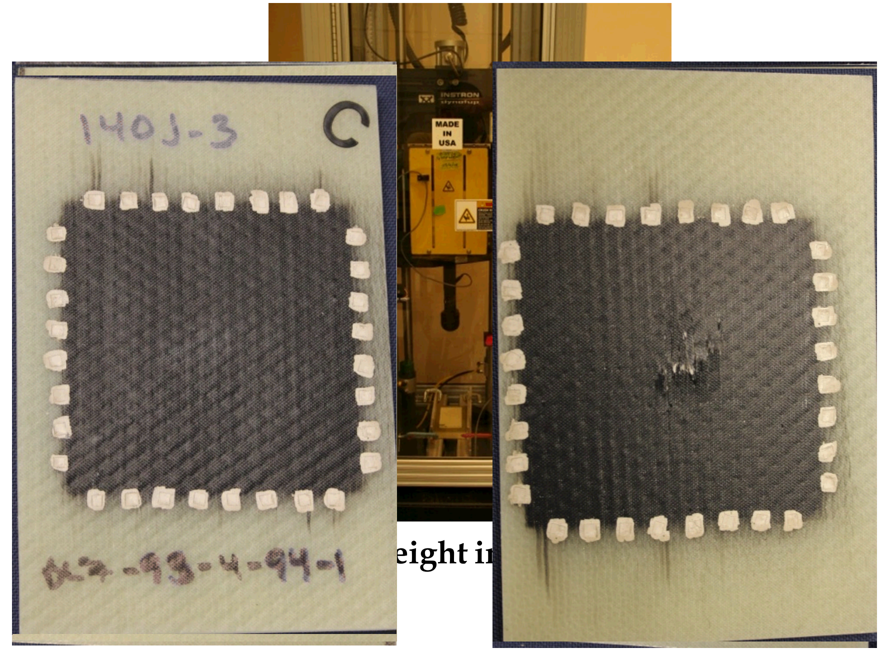

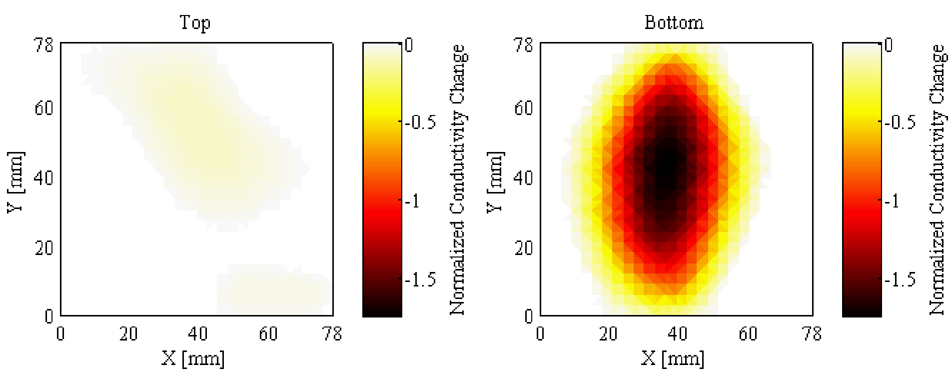

Summary

- Propose a next-generation SHM system
  - Direct in situ damage detection
  - Monitor location and severity of damage
- Embedding multi-modal sensing capabilities
  - Development of MWNT-nanocomposites for SHM
  - Characterized electromechanical response to monotonic and dynamic strain
  - Response to temperature swings
- Outline validation of EIT for damage detection
  - Strain sensitivity
  - Damage sensitivity
  - Impact damage

Thank You!

Sandia National Laboratories

Questions?

Acknowledgements:

UC DAVIS OFFICE OF GRADUATE STUDIES

UC DAVIS COLLEGE OF ENGINEERING

NATIONAL INSTITUTE FOR NANO ENGINEERING (NINE)

CITRIS Center for Information Technology Research in the Interest of Society

National Science Foundation WHERE DISCOVERIES BEGIN